

1 Joint analysis of continental and regional background environments in the  
2 Western Mediterranean: PM<sub>1</sub> and PM<sub>10</sub> concentrations and composition

3  
4 A. Ripoll<sup>1,2\*</sup>, M. C. Minguillón<sup>1</sup>, J. Pey<sup>1,3</sup>, N. Pérez<sup>1</sup>, X. Querol<sup>1</sup>, A.  
5 Alastuey<sup>1</sup>

6 <sup>1</sup>Institute of Environmental Assessment and Water Research (IDAEA-  
7 CSIC), Jordi Girona 18-26, 08034, Barcelona, Spain

8 <sup>2</sup> Department of Astronomy and Meteorology, Faculty of Physics,  
9 University of Barcelona, Martí i Franquès 1, 08028, Barcelona, Spain

10 <sup>3</sup>Now at: Aix-Marseille Université, CNRS, LCE FRE 3416, Marseille,  
11 13331, France

12 \*Correspondence to: A. Ripoll (anna.ripoll@idaea.csic.es)

13

14           **Abstract.** The complete chemical composition of atmospheric particulate  
15 matter (PM<sub>1</sub> and PM<sub>10</sub>) from a continental (Montsec, MSC, 1570 m a.s.l.) and a  
16 regional (Montseny, MSY, 720 m a.s.l) background site in the Western  
17 Mediterranean Basin (WMB) were jointly studied for the first time for a relatively  
18 long-term period (January 2010-March 2013).

19           Differences in average PM<sub>x</sub> concentration and composition between both  
20 sites were attributed to: distance to anthropogenic sources, altitude, and  
21 different influence of atmospheric episodes. All these factors result in a  
22 continental to regional background increase of 4.0 µg m<sup>-3</sup> for PM<sub>10</sub> and 1.1 µg  
23 m<sup>-3</sup> for PM<sub>1</sub> in the WMB. This increase is mainly constituted by organic matter,  
24 sulfate, nitrate and sea salt. However, higher mineral matter concentrations  
25 were measured at the continental background site owing to the higher influence  
26 of long-range transport of dust and dust resuspension.

27           Seasonal variations of aerosol chemical components were ascribed to:  
28 evolution of the planetary boundary layer (PBL) height throughout the year,  
29 variations in the air mass origin, and differences in meteorology. During warmer  
30 months, weak pressure gradients and elevated insolation generate recirculation  
31 of air masses and enhances the development of the PBL, causing the aging of  
32 aerosols and incrementing pollutant concentrations over a large area in the  
33 WMB, including the continental background. This is reflected in a more similar  
34 relative composition and absolute concentrations of continental and regional  
35 background aerosols. Nevertheless, during colder months the thermal  
36 inversions and the lower vertical development of the PBL leave MSC in the free  
37 troposphere most of the time, whereas MSY is more influenced by regional  
38 pollutants accumulated under winter anticyclonic conditions. This results in  
39 much lower concentrations of PM<sub>x</sub> components at the continental background  
40 site with respect to those at the regional background site.

41           The influence of certain atmospheric episodes caused different impacts  
42 at regional and continental scales. When long-range transport from Central and  
43 Eastern Europe and from North Africa occurs, the continental background site is  
44 frequently more influenced, thus indicating a preferential transport of pollutants  
45 at high altitude layers. Conversely, the regional background site was more  
46 influenced by regional processes.

47 Continental and regional aerosol chemical composition from the WMB  
48 revealed: a) high relevance of African dust transport and regional dust  
49 resuspension; b) low biomass burning contribution; c) high organic matter  
50 contribution; d) low summer nitrate concentrations; and e) high aerosol  
51 homogenization in summer.

52

53 **Keywords:** remote, high altitude, mountain, tropospheric aerosols, rural.

54

## 55 **1 Introduction**

56 The influence of atmospheric particulate matter (PM) on the Earth's  
57 radiative budget generates a strong scientific interest because of its effect on  
58 climate. Atmospheric PM interacts with the Earth's climate system by scattering  
59 and absorbing solar radiation (direct climate forcing effect), and by acting as  
60 cloud condensation nuclei (indirect climate forcing effect) (IPCC, 2013).  
61 Aerosols also have adverse effects on air quality (Directive 2008/50/EC) and  
62 human health (WHO, 2013), as well as on ecosystems (e.g. Burkhardt and  
63 Pariyar, 2014). The size distribution of aerosol chemical components is a key  
64 factor in modulating these effects, and provides valuable information on the  
65 aerosol origins and sources. Aerosol chemical composition measurements  
66 carried out at complex sites such as urban areas constrain the assessment of  
67 the origin of regional and long-range transported aerosols, as local sources  
68 prevail. For this reason, measurements performed at a sufficient distance from  
69 large emission sources are needed to determine background conditions and to  
70 evaluate air mass transport effects. Furthermore, an improved understanding of  
71 synoptic and mesoscale meteorological effects is necessary to develop a better  
72 predictive capability of air quality and climate models.

73 Although there is not a well-established definition, continental  
74 background environments can be described as representative of the air quality  
75 of a wide area of hundreds of kilometers, as proposed by Laj et al. (2009), with  
76 the absence of local emissions. However, aerosols found in this type of  
77 environments are not purely natural, the presence of some pollutants in these  
78 sites indicates that they are affected by long-range transport of anthropogenic  
79 emissions, since generally they are isolated from large polluted areas (>50 km)

80 (Putaud et al., 2010). For this reason, these environments are also classified as  
81 remote sites. In many cases the monitoring sites chosen to represent this type  
82 of environments are located in mountaintops over 1000 m above sea level  
83 (a.s.l.), therefore they are also called high altitude sites (Nyeki et al., 1998) or  
84 free troposphere (FT) environments (Andrews et al., 2011). The areas located  
85 at sufficient distance from large anthropogenic sources but frequently within the  
86 planetary boundary (PBL) are classified as regional background environments  
87 (Putaud et al., 2010). These environments are representative of the air quality  
88 of a less extensive area and they are more influenced by regional transport of  
89 polluted air masses than continental background environments.

90         Aerosol chemical characterization has been performed at many locations  
91 across Europe, providing information on PM<sub>10</sub> and PM<sub>2.5</sub> chemical composition  
92 from different types of environments (e.g. Putaud et al., 2010), improving the  
93 knowledge on the variation and trends of PM composition (e.g. Cusack et al.,  
94 2012), and increasing the understanding of PM sources (Belis et al., 2013).  
95 Nevertheless, the PM<sub>1</sub> fraction remains relatively understudied, especially  
96 outside urban areas. Most studies focusing on PM<sub>1</sub> have been carried out within  
97 the PBL whereas measurements at continental background sites in Europe are  
98 scarce and they were mostly taken in short-term measurement campaigns (e.g.  
99 Carbone et al., 2010; Marengo et al., 2006). The study of PM<sub>1</sub> chemical  
100 composition at continental background sites may be necessary to assess the  
101 contribution of regional and long-range transport, since it is in the PM<sub>1</sub> fraction  
102 where most of the anthropogenic constituents are concentrated (Minguillón et  
103 al., 2012; Pérez et al., 2008b).

104         Among the few long-term European studies at continental background  
105 environments, Cozic et al. (2008) investigated the chemical composition of  
106 coarse and PM<sub>1</sub> aerosols for 7 years at the high alpine site of Jungfrauoch  
107 (Switzerland). Bourcier et al. (2012) studied PM<sub>10</sub> and PM<sub>1</sub> water-soluble  
108 inorganic components over one year at the high altitude site of Puy de Dôme  
109 (France). Recently, Carbone et al. (2014) performed a study on long-term  
110 measurements of chemical composition in the continental background  
111 environment of the Southern Europe/Northern Mediterranean. This study was  
112 focused on nocturnal PM<sub>1</sub> chemical composition for 3 years at the high  
113 mountain station of Mt. Cimone (Italy).

114 The Mediterranean region is characterized by particular atmospheric  
115 dynamics strongly influenced by its topography (Jorba et al., 2013; Millan et al.,  
116 1997). Over this region, elevated emissions of anthropogenic pollutants occur,  
117 arrival of natural and anthropogenic aerosols as a result of long-range transport  
118 from Africa and Europe is frequent (Pey et al., 2010, 2013b; Ripoll et al., 2014),  
119 and accumulation and recirculation processes are recurrently observed  
120 (Rodriguez et al., 2002).

121 For these reasons, results of PM<sub>10</sub> and PM<sub>1</sub> chemical characterization  
122 from Montsec (MSC) and Montseny (MSY) Global Atmosphere Watch (GAW)  
123 stations for the period of January 2010-March 2013 are presented in this study.  
124 MSC is representative of the continental background conditions of the Western  
125 Mediterranean Basin (WMB) (Ripoll et al. 2014). This station is located in the FT  
126 most of the time due to its elevation (1570 m a.s.l.); although during the warmer  
127 months that isolation is broken as a result of vertical mixing and mountain  
128 breeze regimes (Ripoll et al. 2014). MSY is a regional background observatory  
129 located in the WMB (720 m a.s.l.) in operation since 2002 (Cusack et al., 2012;  
130 Pérez et al., 2008a) and it is influenced by regional anthropogenic emissions in  
131 specific scenarios (Pérez et al., 2008a; Pey et al., 2010). The record of a  
132 relatively long series of PM<sub>10</sub> and PM<sub>1</sub> concentrations and complete chemical  
133 composition at two different WMB environments has allowed for the  
134 investigation of temporal and spatial aerosol variations in the WMB with focus  
135 on regional and long-range transport processes. Daily and seasonal patterns of  
136 PM<sub>10</sub> and PM<sub>1</sub> concentrations, as well as their major components and trace  
137 elements at MSC and MSY, were investigated. Greater emphasis was placed  
138 on the evaluation of the influence of different meteorological scenarios, with a  
139 focus on the partitioning of the chemical components into different size fractions  
140 in order to discriminate natural and anthropogenic impacts affecting PM<sub>10</sub> and  
141 PM<sub>1</sub>. To the authors' knowledge, no similar studies exist in the literature which  
142 compares continental and regional background environments and their  
143 seasonal variation.

## 144 2 Methodology

### 145 2.1 Monitoring sites and sampling schedule

146 The continental background site was set up in the Montsec (MSC)  
147 mountain range, located in the NE of the Iberian Peninsula (42°3'N, 0°44'E,  
148 1570 m a.s.l.). This station is situated at 50 km to the S of the Axial Pyrenees  
149 and at 140 km to the NW of Barcelona (Fig. S1). A detailed description of this  
150 site can be found in Ripoll et al. (2014).

151 Results from MSC were jointly studied with those simultaneously  
152 obtained at the Montseny (MSY) station, a regional background observatory  
153 located in the Montseny Natural Park (41°19'N, 02°21'E, 720 m a.s.l.), 40 km to  
154 the N-NE of the Barcelona urban area, and 25 km from the Mediterranean coast  
155 (Fig. S1) (Pérez et al., 2008a).

156 At MSC site, 24-h samples of PM<sub>10</sub> and PM<sub>1</sub> were collected every 4 days  
157 on 150 mm quartz micro-fiber filters (Pallflex QAT) using high volume samplers  
158 (30 m<sup>3</sup> h<sup>-1</sup>, MCV CAV-A/MSb) equipped with MCV PM<sub>10</sub> and PM<sub>1</sub> cut-off inlets.  
159 PM<sub>10</sub> and PM<sub>1</sub> sampling began in November 2009 and in March 2011,  
160 respectively. In this work we study the results from January 2010 (March 2011  
161 for PM<sub>1</sub>) to March 2013. In addition to the routine measurements, 5 intensive  
162 campaigns (daily sampling) were performed during Mar-Apr 2011, Jul-Aug  
163 2011, Jan-Feb 2012, Jun-Jul 2012 and Jan-Feb 2013. Overall, 391 and 235  
164 samples of PM<sub>10</sub> and PM<sub>1</sub>, respectively, were collected throughout the study  
165 period, and PM<sub>1-10</sub> concentrations were calculated by the difference of  
166 simultaneous PM<sub>1</sub> and PM<sub>10</sub> daily samples (190 days).

167 At MSY site, 24-h samples of PM<sub>10</sub> and PM<sub>1</sub> were also collected from  
168 January 2010 to March 2013 using high volume samplers (30 m<sup>3</sup> h<sup>-1</sup>, DIGITEL-  
169 DH80) equipped with PM<sub>10</sub> and PM<sub>1</sub> cut-off inlet (also DIGITEL). A total of 351  
170 and 335 samples of PM<sub>10</sub> and PM<sub>1</sub>, respectively, were collected during the  
171 study period, and PM<sub>1-10</sub> samples were calculated for 147 days. In most cases,  
172 sampling days were coincident at MSC and at MSY.

173 2.2 Chemical characterization

174 PM mass concentrations were determined by standard gravimetric  
175 procedures, and complete chemical analysis for all filters was performed  
176 following the procedures proposed by Querol et al. (2001).

177 Acid digestion (HF:HNO<sub>3</sub>:HClO<sub>4</sub>) of 1/4 of each filter was carried out to  
178 determine and quantify major and trace elements by Inductively Coupled  
179 Plasma Mass Spectrometry (ICP-MS, X Series II, THERMO) and Atomic  
180 Emission Spectroscopy (ICP-AES, IRIS Advantage TJA solutions, THERMO).  
181 Few mg of the reference material NIST 1633b were added to 1/4 of laboratory  
182 blank filters to check the accuracy of the analysis of the acidic digestions. One  
183 1/4 of each filter was leached with ultrapure water (miliQ) to determine the  
184 content of Cl<sup>-</sup>, SO<sub>4</sub><sup>2-</sup>, and NO<sub>3</sub><sup>-</sup> by Ion High Performance Liquid Chromatography  
185 (HPLC) using a WATERS ICpak™ anion column with a WATERS 432  
186 conductivity detector, and NH<sub>4</sub><sup>+</sup> concentrations with a Selective Electrode  
187 (MODEL 710 A+, THERMO Orion). A rectangular portion (1.5 cm<sup>2</sup>) of the  
188 remaining filter was used for the analysis of organic carbon (OC) and elemental  
189 carbon (EC) by a SUNSET OCEC analyzer using the EUSAAR 2 protocol  
190 (Cavalli et al., 2010). Moreover, one blank filter was kept for each set of ten  
191 filters. Blank concentrations were subtracted from the total concentration  
192 measured for each sample, thus giving ambient concentrations. To complete  
193 mass balances, the following indirect determinations were obtained: a) CO<sub>3</sub><sup>2-</sup>,  
194 calculated from Ca as CO<sub>3</sub><sup>2-</sup>=1.5\*Ca; b) Al<sub>2</sub>O<sub>3</sub>, calculated from Al as  
195 Al<sub>2</sub>O<sub>3</sub>=1.889\*Al; c) SiO<sub>2</sub>, calculated as SiO<sub>2</sub>=2.5\*Al<sub>2</sub>O<sub>3</sub>, and d) organic matter  
196 (OM) obtained applying a 2.2 factor to the OC concentrations for MSC samples  
197 and a 2.1 factor for MSY samples, following the suggestion from Takahama et  
198 al. (2011). By following these procedures we were able to determine and  
199 quantify the concentrations of major components (OC, EC, SiO<sub>2</sub>, CO<sub>3</sub><sup>2-</sup>, Al<sub>2</sub>O<sub>3</sub>,  
200 Ca, Al, Na, Mg, Fe, K, NO<sub>3</sub><sup>-</sup>, SO<sub>4</sub><sup>2-</sup>, NH<sub>4</sub><sup>+</sup> and Cl<sup>-</sup>) and trace elements (Li, P, Ti,  
201 V, Cr, Mn, Co, Ni, Cu, Zn, As, Se, Rb, Sr, Cd, Sn, Sb, Ba, La, Pb, among  
202 others). Overall, the aforementioned components accounted for 60–90% of the  
203 total PM mass. Most of the undetermined mass was attributed to water not  
204 eliminated during filter conditioning in the presence of hygroscopic species, but  
205 a contribution from sampling artifacts and from the use of factors to determine  
206 CO<sub>3</sub><sup>2-</sup>, SiO<sub>2</sub>, and OM cannot be discarded.

207 At MSC the mineral matter (MM) determination was calculated as:  
208  $MM = CO_3^{2-} + SiO_2 + Al_2O_3 + Ca + Fe + K + nss-Na + Mg + Mn + Ti + P$  [1]  
209 Where nss-Na is the non-sea-salt sodium and it was calculated as nss-  
210  $Na = Al_2O_3 * 0.067$  according to the composition of the mineral particles from the  
211 Sahara given by Moreno et al. (2006), and hence the remaining sodium was  
212 sea-salt sodium ( $ss-Na = Na - nss-Na$ ).  
213 Consequently, the sea salt (SS) determination at MSC was given by:  
214  $SS = Cl^- + ss-Na$  [2]  
215 At MSY, Na concentrations were totally attributed to SS, given that it is  
216 located closer to the sea and in agreement with Pey et al. (2009).

### 217 2.3 Principal component analysis

218 Principal component analysis (PCA) was performed using the software  
219 STATISTICA v10.0. The orthogonal transformation method with Varimax  
220 rotation (Thurston and Spengler, 1985) was employed, retaining principal  
221 components with eigenvalues greater than one. The dataset used for PCA was  
222 comprised of the following PM<sub>10</sub> constituents Cl<sup>-</sup>, NO<sub>3</sub><sup>-</sup>, NH<sub>4</sub><sup>+</sup>, SO<sub>4</sub><sup>2-</sup>, Al<sub>2</sub>O<sub>3</sub>, Ca,  
223 K, Na, Mg, Fe, Li, Ti, V, Cr, Mn, Ni, Cu, Zn, As, Se, Sr, Cd, Sb, Pb, OC and EC.  
224 All days with measurements of PM<sub>10</sub> chemical analysis were included for PCA  
225 analysis, which totalled 390 cases from MSC and 351 cases from MSY. A  
226 typical robust PCA analysis requires at least a dataset with 100 cases. This  
227 technique allowed for the identification of main common groups of trace  
228 elements in PM<sub>10</sub> at the continental and regional background sites.

### 229 2.4 Classification of atmospheric episodes

230 The classification of the atmospheric episodes affecting MSC and MSY  
231 sites on each day of the sampling period was performed following the procedure  
232 described by Ripoll et al. (2014), and the different air mass transport pathways  
233 determined were: 1) Atlantic North (AN), 2) Atlantic North West (ANW), 3)  
234 Atlantic South West (ASW), 4) North Africa (NAF), 5) Mediterranean (MED), 6)  
235 Europe (EU), 7) Winter Regional (WREG, from November to April), and 8)  
236 Summer Regional (SREG, from May to October) (Fig. 1).

237 Additionally, the boundary layer height was calculated at MSC and MSY  
238 sites using the READY model from the NOAA Air Resources Laboratory



239 (<http://www.ready.noaa.gov/READYamet.php>), which is based in meteorological  
240 conditions defining Pasquill stability classes, and uses a resolution grid of 50  
241 km. This was calculated every three hours during the whole period (Fig. S2).  
242 Despite the limited suitability of this type of model for mountainous terrains, the  
243 differences found throughout the year and among different atmospheric  
244 scenarios can be considered as a good approximation of the actual PBL  
245 variations.

### 246 **3 Results and discussion**

#### 247 *3.1 Continental vs. regional background PM concentrations in the Western* 248 *Mediterranean*

249  $PM_{10}$  and  $PM_1$  average concentrations ( $\pm$  standard deviation) measured  
250 at MSC continental background site reached  $11.5 \pm 9.3 \mu\text{g m}^{-3}$  and  $7.1 \pm 3.9 \mu\text{g}$   
251  $\text{m}^{-3}$ , respectively, whereas at MSY regional background site these  
252 concentrations were  $15.5 \pm 7.9 \mu\text{g m}^{-3}$  and  $8.2 \pm 4.1 \mu\text{g m}^{-3}$  (Table S1). Thus,  
253 the continental to regional background increase is estimated in  $4.0 \mu\text{g m}^{-3}$  for  
254  $PM_{10}$  and  $1.1 \mu\text{g m}^{-3}$  for  $PM_1$  in the WMB. This increase is caused by  
255 differences of: a) altitude, b) distance to anthropogenic sources, and c) impact  
256 of atmospheric episodes. The contribution of different aerosol chemical  
257 components to this increment will be discussed in section 3.2.

258 A significant seasonal variation of  $PM_{10}$  and  $PM_1$  mass concentrations  
259 was observed at both sites, with maximum values in summer and minimum in  
260 winter (Fig.2). Comparable seasonal patterns for  $PM_x$  concentrations were  
261 described for MSC (Ripoll et al., 2014) and for other regional and continental  
262 background sites in southern Europe (e.g. Cozic et al., 2008; Querol et al.,  
263 1998; Rodríguez et al., 2003; Tositti et al., 2013). In those studies the seasonal  
264 pattern has been attributed to changes in the air mass origin from summer to  
265 winter, and to the different PBL height between seasons. Moreover, at both  
266 MSC and MSY sites a secondary maximum of  $PM_{10}$  and  $PM_1$  concentrations  
267 was observed in early spring (Fig. 2).

268  $PM_{10}$  concentrations showed a stronger seasonal pattern than  $PM_1$   
269 concentrations at both sites (Fig. 2). This is ascribed to the higher impact of  
270 resuspended and long-range transported dust on the  $PM_{10}$  fraction, both

271 enhanced in summer (see section 3.3), and to the prevalence of the  
272 anthropogenic constituents in PM<sub>1</sub>, whose emissions occur all along the year.

273 Comparison of these results with those from other continental  
274 background sites in Central Europe, such as Puy de Dôme at 1465 m a.s.l. in  
275 France (Bourcier et al., 2012) and Jungfraujoch at 3454 m a.s.l. in Switzerland  
276 (Cozic et al., 2008), shows that PM<sub>10</sub> and PM<sub>1</sub> concentrations were higher at the  
277 continental background site in the WMB (Fig. S3 and Table S1). Such higher  
278 PM<sub>10</sub> and PM<sub>1</sub> concentrations at MSC are related to the increasing role of  
279 Saharan dust particles over this area, as discussed in section 3.3 and in  
280 agreement with Ripoll et al. (2014); and to the more polluted atmosphere in  
281 summer as a result of the air mass recirculation over the WMB (Millan et al.,  
282 1997). By contrast, PM<sub>10</sub> concentrations at the regional background site in the  
283 WMB were lower than those at the rural sites in Switzerland (Gianini et al.,  
284 2012) (Fig. S3 and Table S1), probably because of the specific alpine location  
285 of these sites which hinders pollution dispersion.

286

## 287 3.2 *Continental vs. regional background aerosol chemical composition in the* 288 *Western Mediterranean*

### 289 3.2.1 Average aerosol chemical composition

290 PM<sub>1</sub> was mainly composed of OM at both sites (39% at MSC and 34% at  
291 MSY), followed by sulfate (17 and 21%), ammonium (7 and 6%), MM (5 and  
292 4%), nitrate (3%), SS (1 and 2%), and EC (1 and 2%) (Fig. 3 and Table S1).  
293 The undetermined mass accounted for 27 and 28%. The PM<sub>1-10</sub> fraction mainly  
294 differed in the contribution of MM (55% at MSC and 39% at MSY), whereas the  
295 other components contributed similarly: OM (14 and 15%), nitrate (9 and 11%),  
296 sulfate (5 and 7%), SS (3 and 5%), ammonium (1 and 2%) and EC (0.4 and  
297 1%). The undetermined mass was 20% at MSY and 13% at MSC. The closer  
298 compositional similarities for PM<sub>1</sub> fraction points to the suitability of using PM<sub>1</sub>  
299 as indicator of regional anthropogenic pollution in Europe, and reflects the wider  
300 spatial representativeness of the fine PM.

301 Overall, average absolute concentrations of chemical components were  
302 more similar between MSC and MSY for PM<sub>1</sub> than for the PM<sub>10</sub> (Fig. 3 and

303 Table S1). The PM<sub>1</sub> continental to regional background increase of 1.1 µg m<sup>-3</sup>  
304 was attributed to the higher concentrations of PM<sub>1</sub> sulfate, EC, OM, and some  
305 anthropogenic trace elements (V, Ni, Cu, Zn, and Pb) at the regional  
306 background site. The increase of 4.0 µg m<sup>-3</sup> of PM<sub>10</sub> at MSY with respect to  
307 MSC is attributed to higher concentrations of OM, sulfate, nitrate and SS. These  
308 differences confirm that MSC is located at a sufficient altitude and distance from  
309 large urban/industrial agglomerations to avoid direct anthropogenic influence  
310 and to be considered a continental background site of the WMB. This also  
311 confirms that MSY is more affected by the marine aerosols as it is located  
312 closer to the coast. Nevertheless, MM and MM-related elements (Ti, Mn, Li and  
313 Sr) PM<sub>10</sub> concentrations were higher at the continental background site than at  
314 the regional background site, probably due to the prevalence of long-range dust  
315 transport at higher altitude layers (Sicard et al., 2011), and to the higher dust  
316 resuspension at MSC.

317 In order to provide a global picture of the origin and variability of trace  
318 elements in the study region, a Principal Component Analysis (PCA) was  
319 performed. This exploration permitted the identification of three main common  
320 groups of trace elements in PM<sub>10</sub> at the continental and regional background  
321 sites. Ordered by their contribution to the total mass of trace elements in PM<sub>10</sub>  
322 these groups were: mineral, industrial + road traffic and fuel oil combustion  
323 related elements (Table S2 and Table S3).

324 In the **mineral** group typical crustal elements (Ti, Mn, Li, and Sr) were  
325 included, but also V, Cr, Co, Ni, and As were partially associated with this factor  
326 since these elements, usually attributed to anthropogenic sources, are also  
327 found in clay mineral assemblages. The group for which high loading factors  
328 were obtained for Cu, Zn, As, Cd, Pb, Sb and Sn was associated with  
329 **industrial + road traffic** sources, based on previous studies which identified a)  
330 Pb, Zn, Mn, and Cd as tracers of the influence of industrial activities located in  
331 the surroundings of Barcelona, such as smelters and cement kilns, b) Cu, Sn  
332 and Sb as tracers of non-exhaust vehicle emissions (Amato et al., 2009). These  
333 sources could not be split by the PCA probably because these emissions are  
334 mixed during their transportation from industrial and urban areas to MSY and  
335 MSC. The **fuel oil combustion** group was better identified at MSY than at  
336 MSC, and it was traced by V and Ni. These elements are typical markers of fuel

337 oil combustion, strongly influenced by shipping emissions in the study region  
338 (Minguillón et al., 2014; Pey et al., 2013a).

339 Fig. S3 and S4 and Table S1 shows average concentrations of chemical  
340 components in PM<sub>10</sub> at the continental background site of Puy de Dôme  
341 (Bourcier et al., 2012) and at the rural stations of Payerne and Magadino  
342 (Gianini et al., 2012). Nitrate and ammonium PM<sub>10</sub> concentrations at MSC were  
343 slightly higher than those observed at Puy de Dôme, whereas the  
344 concentrations registered at MSY were lower than those measured at Payerne  
345 and Magadino. The similar sulfate concentrations across Europe in both  
346 continental and regional background areas corroborate that this component can  
347 remain in the atmosphere for long time, homogenizing sulfate concentrations in  
348 Europe. Average PM<sub>10</sub> concentrations of EC and OM in the WMB were lower  
349 than those measured at Payerne and Magadino, probably due to the higher  
350 influence of biomass burning in Central Europe. This is confirmed by the higher  
351 concentrations of the well-known biomass burning tracer potassium (Pio et al.,  
352 2008) registered at the Swiss stations, most of it water soluble (Gianini et al.,  
353 2012). Mineral major (Al+Ca+Mg) and trace (Ti, Sr, La or Ce) elements at MSC  
354 and MSY were recorded in concentrations twice as high as those at Payerne  
355 and Magadino indicating the higher influence of Saharan dust transport and  
356 regional dust resuspension in the Mediterranean area. As expected, a higher  
357 influence of SS particles was observed at MSC and MSY than at Payerne and  
358 Magadino owing to their closer location to the Mediterranean Sea. Conversely,  
359 the highest concentrations of typical anthropogenic trace elements, such as Ni,  
360 Cu, Zn, As, Cd, Sb, and Pb, were recorded at the Swiss stations, with the  
361 exception of V which was higher at the Spanish sites. This can be partially  
362 attributed to a greater influence of emissions from fuel-oil combustion, mostly  
363 from shipping emissions in the Mediterranean region (Pey et al., 2009).

### 364 3.2.2 Partitioning of major and trace components in PM<sub>1</sub> and PM<sub>1-10</sub>

365 In the WMB region **nitrate** showed a prevalent coarse grain size  
366 distribution (Figs. 3 and S5). PM<sub>1-10</sub> nitrate compounds were partially associated  
367 with mineral dust and sea salt particles, since nitric acid and/or some other  
368 nitrogen compounds can react with these particles (Wall et al., 1988; Zhuang et  
369 al., 1999a). The resulting coarse sodium or calcium nitrates particles are much

370 more stable than ammonium nitrate at high temperature and low humidity  
371 (Zhuang et al., 1999b).

372 As expected, **sulfate** was mainly fine at both sites (Figs. 3 and S5),  
373 hence attributed to the presence of ammonium sulfate as deduced by the good  
374 ionic balance fitting between sulfate and ammonium ( $R^2=0.899$ ). Nevertheless,  
375  $PM_{1-10}$  sulfate was also detected at MSC and MSY, and it was partially  
376 attributed to mineral dust and sea salt particles, and partially attributed to the  
377 reaction product between sulfuric acid and/or sulfur dioxide ( $SO_2$ ) and these  
378 natural particles (Wall et al., 1988; Zhuang et al., 1999a).

379 **Ammonium** showed a prevalent fine grain size distribution at the  
380 continental and regional background sites (Figs. 3 and S5). Fine ammonium  
381 was attributed to the presence of both ammonium nitrate and ammonium  
382 sulfate.  $PM_{1-10}$  ammonium is most likely in  $PM_{1-2.5}$  fraction, according to Querol  
383 et al. (2009).

384 **OM** was mainly fine at both sites (Figs. 3 and S5). A high number of  
385 studies have demonstrated the dominant secondary origin of the fine OM  
386 (Jimenez et al., 2009). In the study area, previous works found that secondary  
387 organic aerosols (SOA) accounted for 91% and 55% of the OM at MSY and at  
388 the city of Barcelona, respectively (Minguillón et al., 2011; Mohr et al., 2012).  
389 Therefore, fine OM at MSC is expected to be dominated by SOA, even more  
390 than at MSY given its remote settlement. Furthermore, the presence of OM in  
391  $PM_{1-10}$ , especially in spring and summer, suggests the impact of primary  
392 bioaerosols (Pöschl et al., 2010).

393 Despite **EC** was mainly fine at both sites (Figs. 3 and S5),  $PM_{1-10}$  EC was  
394 also detected, suggesting a partial association between EC and MM by means  
395 of adsorption of anthropogenic pollutants onto dust.

396 As expected, most of the **MM** species and the mineral trace elements  
397 were encountered in the  $PM_{1-10}$  fraction, while the concentrations in  $PM_1$  were  
398 clearly lower at both sites (Figs. 3 and S6 and Table S1). Contrary to the rest of  
399 MM species, K was also abundant in  $PM_1$  fraction and its concentrations were  
400 slightly higher at MSY than those at MSC (Figs. S6 and S7c). This indicates an  
401 additional source origin other than mineral (generally as K-feldspar and illite, a  
402 K-bearing clay mineral), such as biomass burning, especially over the regional  
403 background. The winter DAURE campaign performed in March 2009 revealed

404 that biomass burning emissions accounted for 33% of EC and 22% of OM at  
405 MSY (Minguillón et al., 2011). Nevertheless, these contributions are much lower  
406 than those obtained at other European regions (Pio et al., 2011).

407 **SS** components were found mainly in the PM<sub>1-10</sub> fraction at both sites  
408 (Figs. 3 and S5) as we expected. In the continental background, the lower  
409 variation of SS concentrations as a function of atmospheric episodes reflects  
410 the minor impact of marine aerosols in this continental background area.

411 Most of the **trace elements** showed a prevalent fine grain size  
412 distribution at MSC and MSY (Fig. S8), especially the ones include in the  
413 industrial + road traffic group and in the fuel oil combustion group. V, Cr, Co, Ni,  
414 and As were also found in the PM<sub>1-10</sub> fraction because these elements are also  
415 present in clay mineral assemblages.

416

### 417 *3.3 Atmospheric episodes affecting continental and regional background* 418 *aerosol chemical composition in the Western Mediterranean*

419 The WMB is affected by peculiar atmospheric episodes which influence  
420 aerosol chemical composition. At MSC site higher frequency of Atlantic  
421 advections was detected, whereas MSY site was more influenced by regional  
422 episodes (Fig. 1). However, the seasonal distribution of the main atmospheric  
423 episodes throughout the year is very similar at both sites. The North African  
424 (NAF) episodes were more frequent from March to October (17% and 18% of  
425 the days, at MSC and MSY, respectively), and very often they alternated with  
426 the summer regional (SREG) scenarios (12% and 27% of the days) or both  
427 episodes occurred simultaneously, when the NAF air masses travel at high  
428 altitudes and the stagnation of air masses prevail at surface levels (Escudero et  
429 al., 2005). The winter regional (WREG) scenarios were detected from October  
430 to March (11% and 27% of the days), as well as the European (EU) episodes  
431 (11% and 13% of the days). Air masses from the Atlantic (AN, ANW and ASW)  
432 affected the WMB all along the year (62% and 41% of the days). Conversely,  
433 the Mediterranean (MED) episodes were detected sporadically (4% of the days  
434 at both sites) and therefore conclusions on their characteristics will not be  
435 drawn in the present study. Moreover, the WMB is affected by sporadic large  
436 wildfire events, especially during summer (Cristofanelli et al., 2009).

### 437 3.3.1 North African episodes (NAF)

438 The non-NAF to NAF increase in  $PM_1$  concentrations is estimated in 2.9  
439  $\mu g m^{-3}$  and  $4.6 \mu g m^{-3}$  at MSC and MSY, respectively, whereas this increase in  
440  $PM_{1-10}$  concentrations is estimated in  $14.3 \mu g m^{-3}$  and  $7 \mu g m^{-3}$  (Figs. 4 and 5).  
441 The  $PM_1$  non-NAF to NAF increase was attributed to the increment of  $PM_1$  MM,  
442 sulfate, nitrate, ammonium, OM, and EC (Figs. S5 and S6). In relative  
443 contribution the highest difference in  $PM_1$  concentrations was recorded for MM  
444 at MSC (Fig. 4) thus evidencing that NAF episodes also affect the fine fraction.

445 On the other hand, the higher concentrations of  $PM_{1-10}$  MM under NAF  
446 episodes accounted for the non-NAF to NAF increase of  $PM_{1-10}$  concentrations.  
447 Additionally, average concentrations of trace elements from the mineral group  
448 were higher at the continental background site than at the regional background  
449 site under NAF episodes (Fig. S6). Concentrations of nitrate and sulfate were  
450 high during NAF episodes at both sites when compared with the average (Figs.  
451 S5 and S7b). At MSY concentrations of coarse ammonium and EC also  
452 increased.

453 The higher impact of NAF scenarios on the continental than on the  
454 regional background aerosols in the WMB confirms that African dust travels  
455 preferentially at high altitudes. The concurrent increase of secondary pollutants  
456 (nitrate and sulfate) at MSC demonstrates that dust arrives together with  
457 industrial pollutants, as evidenced at Canary islands by Rodríguez et al. (2011).  
458 The relatively high concentrations of secondary pollutants and EC during NAF  
459 at MSY in  $PM_1$  and  $PM_{1-10}$  can be related to the interaction of dust with  
460 anthropogenic pollutants. During NAF episodes a compression of the PBL is  
461 observed at regional scale (Alastuey et al., 2005; Pandolfi et al., 2013) (Fig.  
462 S9), and a dominance of southern winds during the whole day breaks the  
463 regular sea breeze circulation (Jorba et al., 2013). These processes enhance  
464 the concentration of regional pollutants in the lowest part of the troposphere and  
465 inhibit the sea breeze “clean up” effect.

466 The net contribution of African dust to the  $PM_{10}$  concentrations was  
467 estimated in 16% at MSC and 11% at MSY. This is in agreement with results  
468 presented by Pey et al. (2013b).

469 An example of the impact of NAF episodes on the continental and  
470 regional background aerosols was recorded on 26 March 2011 (Fig. 5b).

471 Backward trajectory for this day clearly showed a North African air mass origin  
472 (Fig. S10) and NAAPS model indicated high dust surface concentrations over  
473 the Iberian Peninsula (Fig. S11). During this episode, dust transport affected  
474 more strongly MSC than MSY, with  $PM_{10}$  MM concentration reaching  $16 \mu\text{g m}^{-3}$   
475 at MSC (more than 5 times higher than the annual average), and  $9 \mu\text{g m}^{-3}$  at  
476 MSY (about 3 times higher than the annual average). At MSC, concentrations of  
477 MM increased simultaneously with those of sulfate (2 times higher than the  
478 annual average), nitrate (3 times) and other anthropogenic elements, such as  
479 Sb and EC, reflecting that dust is transported together with these pollutants.  
480 The increments of absolute concentrations of nitrate, sulfate, Sb and EC were  
481 higher at MSY than MSC probably due to the aforementioned effect of both the  
482 PBL compression and the breeze.

### 483 3.3.2 Summer regional episodes (SREG)

484 The importance of the SREG scenarios in the WMB has been studied in  
485 a number of works (e.g. Escudero et al., 2005; Gangoiti et al., 2001; Millan et  
486 al., 1997; Rodriguez et al., 2002). These episodes take place under weak  
487 barometric gradient and a lack of advections in summer, which causes the  
488 recirculation of air masses over the WMB. Generally, these situations last for  
489 several days, favoring the accumulation of pollutants at regional scale,  
490 increasing the magnitude of convection and aging processes, and enhancing  
491 the dust resuspension and the formation of secondary organic and inorganic  
492 aerosols. For these reasons, under SREG episodes high concentrations of  $PM_1$   
493 and  $PM_{1-10}$  were measured at the regional background site (Fig. 4). The  $PM_1$   
494 increase was attributed to higher concentrations of  $PM_1$  sulfate, OM, EC and  
495 trace elements of industrial + road traffic group, and the  $PM_{1-10}$  increase was  
496 ascribed to higher concentrations of  $PM_{1-10}$  MM, OM, and EC (Figs. S5, S6 and  
497 S8).

498 In spite of the high altitude of MSC, the continental background site was  
499 also affected by this type of episodes due to a higher development of the PBL  
500 over the continental areas (Fig. S9), which favors the transport of anthropogenic  
501 pollutants towards high altitude sites such as MSC, and enhance the dust  
502 resuspension (Figs. 4, S5, S6 and S8).



503 High concentrations of elements such as Ca, Mg, Sr, and Mn during  
504 SREG scenarios (Fig. S6) confirm the local/regional origin of these dust  
505 particles at both sites. However, the ratio of concentrations of these specific  
506 elements with respect to Al during SREG scenarios was higher at MSC  
507 compared to MSY, probably because of the calcareous (richer in Ca, Mg, Sr  
508 and Mn) nature of Montsec range as opposed to the slate and granitic  
509 composition (richer in Al) of Montseny range.

### 510 3.3.3 Winter regional episodes (WREG)

511 The WREG episodes affecting the WMB have been described by Pey et  
512 al. (2010) as winter anticyclonic episodes (WAE), based on a comparison  
513 between urban and regional background sites. In the present study the WREG  
514 episodes showed low concentrations of  $PM_1$  and  $PM_{1-10}$  on average (Fig. 4), but  
515 the chemical composition revealed the higher relative contribution of  
516 anthropogenic sources and the lower relative proportion of natural emissions,  
517 with high concentrations of  $PM_1$  nitrate, ammonium, OM and EC, and the lowest  
518 concentrations of  $PM_{1-10}$  OM and MM, especially at MSY (Figs. S5, S6 and  
519 S7a).

520 The impact of these episodes on the continental and regional  
521 background aerosols can be explained by the persistence of anticyclonic  
522 conditions in the WMB. During these situations the stagnation of air masses  
523 occurs, which increases the pollution around the emission sources (mainly  
524 urban and industrial areas); therefore regional and continental background  
525 areas are presumably free of this anthropogenic pollution. However, the  
526 meteorological conditions (sunny days and thermal inversion) together with the  
527 topography of the WMB (very mountainous) may develop mountain breezes. In  
528 this case, the anthropogenic pollution accumulated over the adjacent valleys,  
529 reaches regional background sites and rarely continental background areas as  
530 intense pollution episodes.

531 Fig. 5d shows an example of a WREG episode affecting the WMB during  
532 the period 14-19 January 2012. Backward trajectory of air masses for these  
533 days corroborate a WREG situation (Fig. S10). During this episode  $PM_{10}$  nitrate,  
534 ammonium, EC and OM concentrations at the regional background site  
535 increased from  $0.2 \mu\text{g m}^{-3}$ ,  $0.2 \mu\text{g m}^{-3}$ ,  $0.2 \mu\text{g m}^{-3}$  and  $3.4 \mu\text{g m}^{-3}$  on 13 January

536 to  $1.3\text{-}5.0\ \mu\text{g m}^{-3}$ ,  $0.6\text{-}1.9\ \mu\text{g m}^{-3}$ ,  $0.2\text{-}0.5\ \mu\text{g m}^{-3}$  and  $3.7\text{-}8.4\ \mu\text{g m}^{-3}$  between 14-  
537 19 January 2012, respectively. Simultaneously, the continental background site  
538 was almost unaffected by such polluted air masses since nitrate, ammonium,  
539 EC and OM concentrations in  $\text{PM}_{10}$  remained between  $0.1\text{-}0.6\ \mu\text{g m}^{-3}$ ,  $0.1\text{-}0.5$   
540  $\mu\text{g m}^{-3}$ ,  $0.05\text{-}0.13\ \mu\text{g m}^{-3}$  and  $2.3\text{-}4.2\ \mu\text{g m}^{-3}$ , respectively.

#### 541 3.3.4 European episodes (EU)

542 During EU episodes air masses from Central and Eastern Europe are  
543 transported towards the WMB crossing the whole continent. This type of  
544 episode is associated with cold meteorological conditions and polluted air  
545 masses (Pey et al., 2010). For this reason, under EU episodes high  
546 concentrations of  $\text{PM}_1$  and  $\text{PM}_{1-10}$  were measured at both sites (Fig. 4). This  
547 increase was attributed to higher concentrations of nitrate, ammonium, OM, EC  
548 and trace elements of industrial + road traffic group at both fractions  $\text{PM}_1$  and  
549  $\text{PM}_{1-10}$ , especially at MSC (Figs. S5 and S8).

550 The higher impact of EU scenarios on the continental background  
551 aerosols than on the regional background aerosols, confirms that the transport  
552 of pollutants occurs preferentially at high altitude layers (between 915-1930 m),  
553 as observed by Sicard et al. (2011).

554 An example of the impact of EU episodes on the continental and regional  
555 background aerosols was recorded on 15 October 2011 (Fig. 5c). During this  
556 episode the air mass remained 3 days over Central Europe before reaching the  
557 WMB, as shown by the backward trajectory (Fig. S4). Under these  
558 meteorological conditions  $\text{PM}_{10}$  nitrate, sulfate, ammonium, EC and OM daily  
559 concentration at MSC reached  $5\ \mu\text{g m}^{-3}$  (6 times higher than the annual  
560 average),  $4\ \mu\text{g m}^{-3}$  (about 3 times higher than the annual average),  $2\ \mu\text{g m}^{-3}$   
561 (more than 4 times higher than the annual average),  $0.3\ \mu\text{g m}^{-3}$  (almost 3 times  
562 higher than the annual average) and  $6.4\ \mu\text{g m}^{-3}$  (about 2 times higher than the  
563 annual average), respectively. Simultaneously, the regional background site  
564 was less affected by this episode as  $\text{PM}_{10}$  nitrate, sulfate, ammonium, EC and  
565 OM concentrations at MSY were  $2.3\ \mu\text{g m}^{-3}$  ( $1\ \mu\text{g m}^{-3}$  higher than the annual  
566 average),  $2.0\ \mu\text{g m}^{-3}$ ,  $0.2\ \mu\text{g m}^{-3}$ ,  $0.2\ \mu\text{g m}^{-3}$  and  $3.2\ \mu\text{g m}^{-3}$ , respectively.

### 567 3.3.5 Atlantic advections (AN, ANW, ASW)

568 The WMB is strongly affected by oceanic air masses owing to the high  
569 influence of Atlantic winds over this region, which is favored by the  
570 displacement of the Azores High westwards or southwards, allowing the  
571 movement of depression systems towards the Mediterranean (Lopez-Bustins et  
572 al., 2008). This type of episodes is associated with increased precipitation and  
573 intense winds, which favors the atmospheric wet-scavenging processes, leading  
574 to the renovation of the regional aged air masses.

575 These meteorological conditions explain why low  $PM_1$  and  $PM_{1-10}$   
576 concentrations were measured under Atlantic advections at both sites (Fig. 4)  
577 and for most of the aerosol chemical components (Figs. S5, S6 and S8).

### 578 3.3.6 Wildfire events

579 Although biomass burning is not a major source in the WMB, some  
580 contribution of biomass burning is observed and partially attributed to wildfires.  
581 Therefore, high concentrations of  $PM_1$  OM and EC during NAF and SREG  
582 episodes (Fig. S5) were partially ascribed to higher frequency of wildfires, since  
583 these episodes very often occur simultaneously.

584 Fig. 5e illustrates the impact of a wildfire on continental and regional  
585 background aerosols in the WMB. This event took place in Eastern Europe on  
586 27-28 March 2012, as shown by the NAAPS model with high smoke surface  
587 concentrations over SE Europe (Fig. S11). Backward trajectory for these days  
588 clearly showed a transport of air masses from SE Europe towards the WMB  
589 (Fig. S10). During this episode, daily  $PM_{10}$  OM and EC concentration at MSY  
590 reached  $7.9 \mu\text{g m}^{-3}$  (almost 2 times higher than the annual average) and  $0.3 \mu\text{g}$   
591  $\text{m}^{-3}$  (1.5 times higher than the annual average), respectively, and at MSC it was  
592  $9.1 \mu\text{g m}^{-3}$  (almost 3 times higher than the annual average) and  $0.3 \mu\text{g m}^{-3}$  (3  
593 times higher than the annual average). Moreover, K concentrations in  $PM_{10}$  at  
594 MSY reached  $0.27 \mu\text{g m}^{-3}$  (2 times higher than the annual average), with a  
595 prevalent fine partitioning ( $PM_1/PM_{10}=0.55$ ), instead of its main coarse  
596 occurrence ( $PM_1/PM_{10}=0.28$ ) during NAF episodes, which confirms the biomass  
597 burning origin.

598

599 3.4 Seasonal variation of continental and regional background aerosol  
600 chemical composition in the Western Mediterranean

601 In addition to the atmospheric episodes discussed above, the aerosols in  
602 the WMB are also affected by the different evolution of the PBL height and  
603 differences in the meteorological parameters throughout the year. In the warmer  
604 months (April-September) the development of the PBL at MSC is much more  
605 relevant than that at MSY (Figs. S2 and S9) owing to the higher convection at  
606 the continental background sites (Rodriguez et al., 2002), and to the higher  
607 cooling effect from the sea breeze at the regional background sites. On the  
608 other hand, in the colder months (October-March) the lower vertical  
609 development of the PBL at the inland sites leaves MSC in the FT on most days,  
610 whereas the regional background site is located most of the day within the PBL  
611 (Fig. S2).

612 **Nitrate** concentrations decreased in summer at both sites, especially in  
613 PM<sub>1</sub> (Fig. 6) (2 and 3 times lower than the winter concentrations at MSC and  
614 MSY, respectively). This decrease was attributed to the high volatility of  
615 ammonium nitrate (Pey et al., 2009) at low humidity and high temperature  
616 (Zhuang et al., 1999b). During the colder months higher nitrate concentrations  
617 are associated to WREG episodes at MSY and to EU episodes at MSC, with  
618 the exception of the November-to-January period, when MSC is mostly within  
619 the FT and therefore low nitrate concentrations were registered.

620 **Sulfate** showed similar seasonal variations at both sites and relatively  
621 similar absolute concentrations, with the highest values during the warmer  
622 months (3 and 2 times higher than the winter concentrations at MSC and MSY,  
623 respectively) (Fig. 6). The squared Pearson correlation coefficient between the  
624 daily sulfate concentrations at MSC and MSY was 0.71. This similarity reflects  
625 the high stability of sulfate and its longer residence time in the atmosphere  
626 resulting in a homogeneous sulfate concentration in the WMB. The summer  
627 maximum was likely due to the higher photochemistry in the atmosphere that  
628 enhances the SO<sub>2</sub> oxidation (6% h<sup>-1</sup> in summer vs <1% h<sup>-1</sup> in winter, Querol et  
629 al., 1999), and to the accumulation of pollutants over the WMB as a result of the  
630 SREG and NAF episodes. Additionally, regional background sulfate aerosols in  
631 summer could be affected by the transport of shipping emissions from the  
632 Mediterranean to the continental areas, due to the more intense sea breeze

633 circulation at MSY. The lower concentrations during the colder months were  
634 attributed to the lower rate of SO<sub>2</sub> oxidation (Querol et al., 1999), and at MSC to  
635 the FT conditions.

636 **Ammonium** concentrations did not follow a clear seasonal pattern (Fig.  
637 6) due to its association with both sulfate and nitrate.

638 **Organic matter** concentrations followed a similar seasonal variation at  
639 both sites, with the highest values during the warmer months (1.8 and 1.5 times  
640 higher than the winter concentrations at MSC and MSY, respectively) (Fig. 6).  
641 The summer maximum was due to: 1) the higher temperature and  
642 photochemistry in the atmosphere that enhances the formation of SOA; 2) the  
643 accumulation of pollutants over the WMB owing to the occurrence of SREG and  
644 NAF episodes; 3) the greater biogenic emissions from vegetation (Seco et al.,  
645 2011); and 4) the higher frequency of wildfires. Furthermore, at MSY a  
646 secondary maximum of OM concentrations occurred in October-March linked to  
647 the occurrence of WREG episodes. The continental background site was less  
648 affected by this type of episodes, since MSC is mostly within the FT in winter.

649 **Elemental carbon** showed high concentrations in the warmer months at  
650 MSC and a less marked seasonal variation at MSY (Fig. 6). The smoother  
651 seasonal variation at MSY reflects the regional anthropogenic influence on the  
652 levels of this component, since anthropogenic emissions occur all along the  
653 year. The higher summer EC concentrations at both sites (more elevated at  
654 MSY) were attributed to the impact of the SREG and NAF episodes, and to the  
655 higher occurrence of wildfires. Additionally, at MSY high concentrations of EC in  
656 summer may be caused by the higher transport of shipping emissions. The  
657 increase of EC during the colder months was not registered simultaneously at  
658 both environments (Fig. 6) because at the regional background site it was  
659 attributed to the impact of WREG episodes, whereas at the continental  
660 background site it was associated with EU episodes.

661 **Mineral matter** concentrations and mineral trace elements in the WMB  
662 are driven by the local and regional dust resuspension and by the contribution  
663 of African dust outbreaks, both enhanced in the warmer months. Consequently,  
664 the highest values were measured in summer and the lowest in winter, with  
665 sporadic high concentrations in March-April (Figs. 6 and 7).

666 **Trace elements** concentrations of the industrial + road traffic group  
667 showed low variations, especially at MSY (Fig. 7), since anthropogenic  
668 emissions occur all along the year. Fuel oil combustion elements showed a  
669 marked seasonal pattern at both sites, with the highest values in summer (Fig.  
670 7) due to the higher shipping emissions and the more frequent and intense sea  
671 breeze circulation, which enhances the transport of air masses from the  
672 Mediterranean Sea.

#### 673 **4 Conclusions**

674 Aerosol chemical characterization ( $PM_1$ ,  $PM_{1-10}$  and  $PM_{10}$ ) and its time  
675 variation were studied during January 2010-March 2013 simultaneously at a  
676 continental (Montsec, MSC) and a regional (Montseny, MSY) background site in  
677 the Western Mediterranean Basin (WMB).

678 In this particular region of the WMB, the continental to regional  
679 background increase was estimated to be  $4.0 \mu\text{g m}^{-3}$  for  $PM_{10}$  and  $1.1 \mu\text{g m}^{-3}$  for  
680  $PM_1$ . Relative chemical composition and absolute concentrations of  $PM_X$   
681 showed very similar values at both environments, especially in  $PM_1$ , in spite of  
682 their altitudinal and longitudinal differences. The similarities are more  
683 pronounced in the warmer months, when recirculation processes at a regional  
684 scale are recurrent in the WMB, and a strong development of the PBL occurs  
685 over continental areas, favoring the transport of anthropogenic pollutants  
686 towards remote sites such as MSC. These processes cause a homogenization  
687 of  $PM_1$  concentration and composition through the region, allowing us to  
688 consider  $PM_1$  as a more suitable indicator of anthropogenic impact than  $PM_{10}$ .  
689 Moreover, the higher temperature and solar radiation in the warmer months  
690 augments atmospheric photochemistry, promoting the formation of secondary  
691 inorganic and organic aerosols and thus incrementing markedly the  
692 concentration of certain components such as sulfate and OM. Additionally, sea  
693 breeze circulation is enhanced, favoring the transport of shipping emissions  
694 from the Mediterranean to the continental areas increasing the concentrations  
695 of sulfate, EC, and fuel oil combustion-related trace elements, especially at the  
696 regional background since it is located closer to the coast. Furthermore, the  
697 occurrence of wildfires across the WMB increases in summer, which contributes  
698 to an extra increment of the OM and EC concentrations. Conversely, nitrate is

699 not abundant in summer due to the high volatility of ammonium nitrate at high  
700 temperatures and low humidity. In the colder months the lower vertical  
701 development of the PBL leaves MSC in the FT on most days, whereas MSY is  
702 frequently located within the PBL due to its lower elevation. As a result, very low  
703 concentrations of all chemical components are recorded at MSC in winter, while  
704 MSY is regularly affected by nearby polluted air masses, which enhanced the  
705 concentrations of  $PM_x$  components.

706         The seasonal variation of major and trace  $PM_x$  components was also  
707 governed by changes in the air mass origin from summer to winter. Whereas  
708 southern flows and regional recirculation episodes are more frequent in  
709 summer, Atlantic advections and northeastern winds from mainland Europe are  
710 more common in winter. As a result, African dust outbreaks and regional dust  
711 resuspension increase MM concentrations over the WMB in the warmer  
712 months. This MM increase affects both  $PM_1$  and  $PM_{1-10}$  and it is frequently more  
713 pronounced at MSC, since long-range transport of dust occurs preferentially at  
714 high altitude layers and dust resuspension is enhanced by the drier surface and  
715 higher convection at this site. During NAF episodes concentrations of nitrate  
716 and sulfate also increase, demonstrating that dust arrives together with  
717 industrial pollutants. Moreover, a compression of the PBL and a change in the  
718 wind regime towards a permanent southern flow, increments the concentrations  
719 of regional pollutants (sulfate, EC and industrial and traffic tracers) in the lowest  
720 part of the troposphere. Regional recirculation of air masses (SREG episodes)  
721 also accounts for the accumulation of airborne particulates, increasing the  
722 concentrations of sulfate, OM, EC, industrial, traffic, and fuel oil combustion  
723 tracers at both continental and regional background environments.

724         In the colder months, the predominance of clean Atlantic advections  
725 prevents the accumulation of regional pollution, and consequently reduces the  
726 concentration of all chemical components at both sites. However, the sporadic  
727 transport of polluted air masses from Central and Eastern Europe towards the  
728 WMB increases the concentrations of nitrate, OM, EC, and industrial and traffic-  
729 related trace elements. The impact of these polluted air masses on the  
730 concentrations of  $PM_x$  components is usually higher in the continental  
731 background, since this transport from Europe occurs preferentially at high  
732 altitude layers. Occasionally, intense peaks of nitrate, OM and EC are

733 measured at the regional background site during the winter anticyclonic  
734 episodes (WREG). These stagnant situations cause the accumulation of  
735 pollutants around the emission sources (such as the Barcelona metropolitan  
736 area), and pollutants can be transported towards relatively nearby areas under  
737 favorable conditions. The distance from MSC to large anthropogenic sources  
738 and its altitude are restricting factors for the occurrence of this process.

739 Finally, the comparison of these results with those from other continental  
740 and regional background sites in Central Europe shows that African dust  
741 transport and regional dust resuspension are much more important in the  
742 Western Mediterranean area. The net contribution of African dust to the PM<sub>10</sub>  
743 concentrations was estimated in 16% at MSC and 11% at MSY. This is  
744 reflected in more elevated concentrations of mineral elements across the  
745 Mediterranean, with the only exception of potassium, higher in Central Europe  
746 due to the contribution of biomass burning emissions. The surprising similar  
747 sulfate concentrations across Europe in both continental and regional  
748 background environments is probably linked to the long residence time of  
749 sulfate aerosols in the atmosphere. On the contrary, nitrate and ammonium  
750 showed different concentrations as a function of site, and nitrate maximum  
751 concentration was observed in winter in the WMB whereas in the Central  
752 Europe continental environments it was measured in summer. Moreover, the  
753 highest concentrations of typical anthropogenic trace elements were recorded  
754 at some European rural environments, with the exception of V which was higher  
755 in the Mediterranean area due to the greater influence of shipping emissions.

756 The concurrent monitoring of aerosols properties in continental and  
757 regional background sites in the WMB provides a complete picture of the  
758 aerosol phenomenology of this region. In view of the relatively high  
759 concentrations of atmospheric aerosols from a variety of natural and  
760 anthropogenic sources, and taking into account the importance of atmospheric  
761 processes. The simultaneous characterization of atmospheric aerosols at  
762 continental and regional background sites feeds with valuable information policy  
763 makers, and air quality and climate models.

764

765 *Acknowledgements.* This study was supported by the Ministry of  
766 Economy and Competitiveness and FEDER funds under the PRISMA



767 (CGL2012-39623-C02-1) and CARIATI (CGL2008-06294/CLI) projects, and by  
768 the Generalitat de Catalunya (AGAUR 2009 SGR8 and the DGQA). The  
769 research received funding from the European Union Seventh Framework  
770 Programme (FP7/ 2007-2013) ACTRIS under grant agreement n° 262254. The  
771 authors would like to extend their gratitude to the personnel from the COU and  
772 the OAdM. We would also like to express our gratitude to the NOAA Air  
773 Resources Laboratory (ARL) for the provision of the HYSPLIT transport and  
774 dispersion model, and boundary layer height calculation, used in this  
775 publication.

## 776 **References**

777 Alastuey, A., Querol, X., Castillo, S., Escudero, M., Avila, A., Cuevas, E.,  
778 Torres, C., Romero, P., Exposito, F. and Garcia, O.: Characterisation of TSP  
779 and PM<sub>2.5</sub> at Izaña and Sta. Cruz de Tenerife (Canary Islands, Spain)  
780 during a Saharan Dust Episode (July 2002), *Atmos. Environ.*, 39, 4715–  
781 4728, doi:10.1016/j.atmosenv.2005.04.018, 2005.

782 Amato, F., Pandolfi, M., Escrig, A., Querol, X., Alastuey, A., Pey, J., Perez, N.  
783 and Hopke, P. K.: Quantifying road dust resuspension in urban environment  
784 by Multilinear Engine: A comparison with PMF<sub>2</sub>, *Atmos. Environ.*, 43, 2770–  
785 2780, doi:10.1016/j.atmosenv.2009.02.039, 2009.

786 Andrews, E., Ogren, J. A., Bonasoni, P., Marinoni, A., Cuevas, E., Rodríguez,  
787 S., Sun, J. Y., Jaffe, D. A., Fischer, E. V., Baltensperger, U., Weingartner,  
788 E., Coen, M. C., Sharma, S., Macdonald, A. M., Leaitch, W. R., Lin, N.-H.,  
789 Laj, P., Arsov, T., Kalapov, I., Jefferson, A. and Sheridan, P.: Climatology of  
790 aerosol radiative properties in the free troposphere, *Atmos. Res.*, 102, 365–  
791 393, doi:10.1016/j.atmosres.2011.08.017, 2011.

792 Belis, C. A., Karagulian, F., Larsen, B. R. and Hopke, P. K.: Critical review and  
793 meta-analysis of ambient particulate matter source apportionment using  
794 receptor models in Europe, *Atmos. Environ.*, 69, 94–108,  
795 doi:10.1016/j.atmosenv.2012.11.009, 2013.

796 Bourcier, L., Sellegri, K., Chausse, P., Pichon, J. M. and Laj, P.: Seasonal  
797 variation of water-soluble inorganic components in aerosol size-segregated  
798 at the puy de Dôme station (1,465 m.a.s.l.), France, *J. Atmos. Chem.*, 69,  
799 47–66, doi:10.1007/s10874-012-9229-2, 2012.

800 Burkhardt, J. and Pariyar, S.: Particulate pollutants are capable to “degrade”  
801 epicuticular waxes and to decrease the drought tolerance of Scots pine  
802 (*Pinus sylvestris* L.), *Environ. Pollut.*, 184, 659–67,  
803 doi:10.1016/j.envpol.2013.04.041, 2014.

- 804 Carbone, C., Decesari, S., Mircea, M., Giulianelli, L., Finessi, E., Rinaldi, M.,  
805 Fuzzi, S., Marinoni, a., Duchi, R., Perrino, C., Sargolini, T., Vardè, M.,  
806 Sprovieri, F., Gobbi, G. P., Angelini, F. and Facchini, M. C.: Size-resolved  
807 aerosol chemical composition over the Italian Peninsula during typical  
808 summer and winter conditions, *Atmos. Environ.*, 44, 5269–5278,  
809 doi:10.1016/j.atmosenv.2010.08.008, 2010.
- 810 Carbone, C., Decesari, S., Paglione, M., Giulianelli, L., Rinaldi, M., Marinoni, A.,  
811 Cristofanelli, P., Diodato, A., Bonasoni, P., Fuzzi, S. and Facchini, M. C.:  
812 3-year chemical composition of free tropospheric PM1 at the Mt. Cimone  
813 GAW global station – South Europe – 2165 m a.s.l., *Atmos. Environ.*, 87,  
814 218–227, doi:10.1016/j.atmosenv.2014.01.048, 2014.
- 815 Cavalli, F., Viana, M., Yttri, K. E., Genberg, J. and Putaud, J. P.: Toward a  
816 standardised thermal-optical protocol for measuring atmospheric organic  
817 and elemental carbon: the EUSAAR protocol, *Atmos. Meas. Tech.*, 3, 79–  
818 89, doi:10.5194/amt-3-79-2010, 2010.
- 819 Cozic, J., Verheggen, B., Weingartner, E., Crosier, J., Bower, K. N., Flynn, M.,  
820 Coe, H., Henning, S., Steinbacher, M., Henne, S., Collaud Coen, M.,  
821 Petzold, a. and Baltensperger, U.: Chemical composition of free  
822 tropospheric aerosol for PM1 and coarse mode at the high alpine site  
823 Jungfraujoch, *Atmos. Chem. Phys.*, 8, 407–423, doi:10.5194/acp-8-407-  
824 2008, 2008.
- 825 Cristofanelli, P., Marinoni, A., Arduini, J., Bonaf, U., Calzolari, F., Colombo, T.,  
826 Decesari, S., Duchi, R., Facchini, M. C., Fierli, F., Finessi, E., Maione, M.,  
827 Chiari, M., Calzolari, G., Messina, P., Orlandi, E., Roccato, F. and Bonasoni,  
828 P.: Significant variations of trace gas composition and aerosol properties at  
829 Mt . Cimone during air mass transport from North Africa – contributions from  
830 wildfire emissions and mineral dust, *Atmos. Chem. Phys.*, 9, 4603–4619,  
831 doi: 10.5194/acp-9-4603-2009, 2009.
- 832 Cusack, M., Alastuey, A., Pérez, N., Pey, J. and Querol, X.: Trends of  
833 particulate matter (PM2.5) and chemical composition at a regional  
834 background site in the Western Mediterranean over the last nine years  
835 (2002–2010), *Atmos. Chem. Phys.*, 12, 8341–8357, doi:10.5194/acp-12-  
836 8341-2012, 2012.
- 837 Cusack, M., Pérez, N., Pey, J., Wiedensohler, A., Alastuey, A. and Querol, X.:  
838 Variability of sub-micrometer particle number size distributions and  
839 concentrations in the Western Mediterranean regional background, *Tellus B*,  
840 65, 1–19, doi: 10.3402/tellusb.v65i0.19243, 2013.
- 841 EC, 2008, Directive 2008/50/EC of the European Parliament and of the Council  
842 of 21 May 2008 on ambient air quality and cleaner air for Europe (OJ L 152,  
843 11.6.2008, p. 1–44).[http://eur-](http://eur-x.europa.eu/LexUriServ/LexUriServ.do?uri=OJ:L:2008:152:0001:0044:EN:P)  
844 [x.europa.eu/LexUriServ/LexUriServ.do?uri=OJ:L:2008:152:0001:0044:EN:P](http://eur-x.europa.eu/LexUriServ/LexUriServ.do?uri=OJ:L:2008:152:0001:0044:EN:P)  
845 [DF](http://eur-x.europa.eu/LexUriServ/LexUriServ.do?uri=OJ:L:2008:152:0001:0044:EN:P)

- 846 Escudero, M., Castillo, S., Querol, X., Avila, A., Alarco, M., Alastuey, A.,  
847 Cuevas, E. and Rodríguez, S.: Wet and dry African dust episodes over  
848 eastern Spain, *J. Geophys. Res.*, 110, D18S08, doi:10.1029/2004JD004731,  
849 2005.
- 850 Gangoiti, G., Millan, M. M., Salvador, R. and Mantilla, E.: Long-range transport  
851 and re-circulation of pollutants in the western Mediterranean during the  
852 project Regional Cycles of Air Pollution in the West-Central Mediterranean  
853 Area, *Atmos. Environ.*, 35, 6267–6276, doi:10.1016/S1352-2310(01)00440-  
854 X, 2001.
- 855 Gianini, M. F. D., Gehrig, R., Fischer, A., Ulrich, A., Wichser, A. and Hueglin, C.:  
856 Chemical composition of PM<sub>10</sub> in Switzerland: An analysis for 2008/2009  
857 and changes since 1998/1999, *Atmos. Environ.*, 54, 97–106,  
858 doi:10.1016/j.atmosenv.2012.02.037, 2012.
- 859 IPCC 2013 in: *Climate Change 2013: The Physical Science Basis (Contribution*  
860 *of Working Group I to the Fifth Assessment Report of the Intergovernmental*  
861 *Panel on Climate Change)* edited by: Myhre, G., Shindell, D., Breon, F.-M.,  
862 Collins, W., Fuglestvedt, J., Huang, J., Koch, D., Lamarque, J.-F., Lee, D.,  
863 Mendoza, B., Nakajima, T., Robock, A., Stephens, G., Takemura, T., and H,  
864 Z. Cambridge Univ. Press, UK and New York, USA, 2013.
- 865 Jimenez, J. L., Canagaratna, M. R., Donahue, N. M., Prevot, A. S. H., Zhang,  
866 Q., Kroll, J. H., DeCarlo, P. F., Allan, J. D., Coe, H., Ng, N. L., Aiken, A. C.,  
867 Docherty, K. S., Ulbrich, I. M., Grieshop, A. P., Robinson, A. L., Duplissy, J.,  
868 Smith, J. D., Wilson, K. R., Lanz, V. A., Hueglin, C., Sun, Y. L., Tian, J.,  
869 Laaksonen, A., Raatikainen, T., Rautiainen, J., Vaattovaara, P., Ehn, M.,  
870 Kulmala, M., Tomlinson, J. M., Collins, D. R., Cubison, M. J., Dunlea, E. J.,  
871 Huffman, J. A., Onasch, T. B., Alfarra, M. R., Williams, P. I., Bower, K.,  
872 Kondo, Y., Schneider, J., Drewnick, F., Borrmann, S., Weimer, S.,  
873 Demerjian, K., Salcedo, D., Cottrell, L., Griffin, R., Takami, A., Miyoshi, T.,  
874 Hatakeyama, S., Shimono, A., Sun, J. Y., Zhang, Y. M., Dzepina, K.,  
875 Kimmel, J. R., Sueper, D., Jayne, J. T., Herndon, S. C., Trimborn, A. M.,  
876 Williams, L. R., Wood, E. C., Middlebrook, A. M., Kolb, C. E., Baltensperger,  
877 U. and Worsnop, D. R.: Evolution of organic aerosols in the atmosphere.,  
878 *Science*, 326, 1525–1529, doi:10.1126/science.1180353, 2009.
- 879 Jorba, O., Pandolfi, M., Spada, M., Baldasano, J. M., Pey, J., Alastuey, A.,  
880 Arnold, D., Sicard, M., Artiñano, B., Revuelta, M. A. and Querol, X.:  
881 Overview of the meteorology and transport patterns during the DAURE field  
882 campaign and their impact to PM observations, *Atmos. Environ.*, 77, 607–  
883 620, doi:10.1016/j.atmosenv.2013.05.040, 2013.
- 884 Laj, P., Klausen, J., Bilde, M., Plaß-Duelmer, C., Pappalardo, G., Clerbaux, C.,  
885 Baltensperger, U., Hjorth, J., Simpson, D., Reimann, S., Coheur, P.-F.,  
886 Richter, A., De Mazière, M., Rudich, Y., McFiggans, G., Torseth, K.,  
887 Wiedensohler, A., Morin, S., Schulz, M., Allan, J. D., Attié, J.-L., Barnes, I.,  
888 Birmili, W., Cammas, J. P., Dommen, J., Dorn, H.-P., Fowler, D., Fuzzi, S.,  
889 Glasius, M., Granier, C., Hermann, M., Isaksen, I. S. A., Kinne, S., Koren, I.,

- 890 Madonna, F., Maione, M., Massling, A., Moehler, O., Mona, L., Monks, P. S.,  
891 Müller, D., Müller, T., Orphal, J., Peuch, V.-H., Stratmann, F., Tanré, D.,  
892 Tyndall, G., Abo Riziq, A., Van Roozendaal, M., Villani, P., Wehner, B., Wex,  
893 H. and Zardini, A. A.: Measuring atmospheric composition change, *Atmos.*  
894 *Environ.*, 43, 5351–5414, doi:10.1016/j.atmosenv.2009.08.020, 2009.
- 895 Lopez-Bustins, J.-A., Martin-Vide, J. and Sanchez-Lorenzo, A.: Iberia winter  
896 rainfall trends based upon changes in teleconnection and circulation  
897 patterns, *Glob. Planet. Change*, 63, 171–176,  
898 doi:10.1016/j.gloplacha.2007.09.002, 2008.
- 899 Marenco, F., Bonasoni, P., Calzolari, F., Ceriani, M., Chiari, M., Cristofanelli, P.,  
900 D’Alessandro, A., Fermo, P., Lucarelli, F., Mazzei, F., Nava, S.,  
901 Piazzalunga, A., Prati, P., Valli, G. and Vecchi, R.: Characterization of  
902 atmospheric aerosols at Monte Cimone, Italy, during summer 2004: Source  
903 apportionment and transport mechanisms, *J. Geophys. Res.*, 111, D24202,  
904 doi:10.1029/2006JD007145, 2006.
- 905 Millan, M. M., Salvador, R., Mantilla, E. and Kallos, G.: Photooxidant dynamics  
906 in the Mediterranean basin in summer: Results from European research  
907 projects, *J. Geophys. Res.*, 102, 8811–8823, 1997.
- 908 Minguillón, M. C., Cirach, M., Hoek, G., Brunekreef, B., Tsai, M., de Hoogh, K.,  
909 Jedynska, A., Kooter, I. M., Nieuwenhuijsen, M. and Querol, X.: Spatial  
910 variability of trace elements and sources for improved exposure assessment  
911 in Barcelona, *Atmos. Environ.*, 48, 268–281,  
912 doi:10.1016/j.atmosenv.2014.02.047, 2014.
- 913 Minguillón, M. C., Perron, N., Querol, X., Szidat, S., Fahrni, S. M., Alastuey, A.,  
914 Jimenez, J. L., Mohr, C., Ortega, A. M., Day, D. A., Lanz, V. A., Wacker, L.,  
915 Reche, C., Cusack, M., Amato, F., Kiss, G., Hoffer, A., Decesari, S., Moretti,  
916 F., Hillamo, R., Teinilä, K., Seco, R., Peñuelas, J., Metzger, A., Schallhart,  
917 S., Müller, M., Hansel, A., Burkhardt, J. F., Baltensperger, U. and Prévôt, A.  
918 S. H.: Fossil versus contemporary sources of fine elemental and organic  
919 carbonaceous particulate matter during the DAURE campaign in Northeast  
920 Spain, *Atmos. Chem. Phys.*, 11, 23573–23618, doi:10.5194/acp-11-12067-  
921 2011, 2011.
- 922 Minguillón, M. C., Querol, X., Baltensperger, U. and Prévôt, A. S. H.: Fine and  
923 coarse PM composition and sources in rural and urban sites in Switzerland:  
924 local or regional pollution?, *Sci. Total Environ.*, 427–428, 191–202,  
925 doi:10.1016/j.scitotenv.2012.04.030, 2012.
- 926 Mohr, C., DeCarlo, P. F., Heringa, M. F., Chirico, R., Slowik, J. G., Richter, R.,  
927 Reche, C., Alastuey, A., Querol, X., Seco, R., Peñuelas, J., Jiménez, J. L.,  
928 Crippa, M., Zimmermann, R., Baltensperger, U. and Prévôt, A. S. H.:  
929 Identification and quantification of organic aerosol from cooking and other  
930 sources in Barcelona using aerosol mass spectrometer data, *Atmos. Chem.*  
931 *Phys.*, 12, 1649–1665, doi:10.5194/acp-12-1649-2012, 2012.

- 932 Moreno, T., Querol, X., Castillo, S., Alastuey, A., Cuevas, E., Herrmann, L.,  
933 Mounkaila, M., Elvira, J. and Gibbons, W.: Geochemical variations in aeolian  
934 mineral particles from the Sahara-Sahel Dust Corridor., *Chemosphere*, 65,  
935 261–70, doi:10.1016/j.chemosphere.2006.02.052, 2006.
- 936 Nyeki, S., Baltensperger, U., Colbeck, I., Jost, D. T., Weingartner, E. and G, H.  
937 W.: The Jungfrauoch high-alpine research station (3454 m) as a  
938 background clean continental site for the measurement of aerosol  
939 parameters, 103, 6097–6107, 1998.
- 940 Pandolfi, M., Martucci, G., Querol, X., Alastuey, A., Wilsenack, F., Frey, S.,  
941 O'Dowd, C. D. and Dall'Osto, M.: Continuous atmospheric boundary layer  
942 observations in the coastal urban area of Barcelona during SAPUSS, *Atmos.*  
943 *Chem. Phys.*, 13, 4983–4996, doi:10.5194/acp-13-4983-2013, 2013.
- 944 Pérez, N., Pey, J., Castillo, S., Viana, M., Alastuey, A. and Querol, X.:  
945 Interpretation of the variability of levels of regional background aerosols in  
946 the Western Mediterranean., *Sci. Total Environ.*, 407, 527–40,  
947 doi:10.1016/j.scitotenv.2008.09.006, 2008a.
- 948 Pérez, N., Pey, J., Querol, X., Alastuey, A., López, J. M. and Viana, M.:  
949 Partitioning of major and trace components in PM<sub>10</sub>–PM<sub>2.5</sub>–PM<sub>1</sub> at an  
950 urban site in Southern Europe, *Atmos. Environ.*, 42, 1677–1691,  
951 doi:10.1016/j.atmosenv.2007.11.034, 2008b.
- 952 Pey, J., Pérez, N., Castillo, S., Viana, M., Moreno, T., Pandolfi, M., López-  
953 Sebastián, J. M., Alastuey, A. and Querol, X.: Geochemistry of regional  
954 background aerosols in the Western Mediterranean, *Atmos. Res.*, 94, 422–  
955 435, doi:10.1016/j.atmosres.2009.07.001, 2009.
- 956 Pey, J., Pérez, N., Querol, X., Alastuey, A., Cusack, M. and Reche, C.: Intense  
957 winter atmospheric pollution episodes affecting the Western Mediterranean.,  
958 *Sci. Total Environ.*, 408, 1951–1959, doi:10.1016/j.scitotenv.2010.01.052,  
959 2010.
- 960 Pey, J., Pérez, N., Cortés, J., Alastuey, A. and Querol, X.: Chemical fingerprint  
961 and impact of shipping emissions over a western Mediterranean metropolis:  
962 Primary and aged contributions, *Sci. Total Environ.*, 497–507,  
963 doi:10.1016/j.scitotenv.2013.06.061, 2013a.
- 964 Pey, J., Querol, X., Alastuey, A., Forastiere, F. and Stafoggia, M.: African dust  
965 outbreaks over the Mediterranean Basin during 2001–2011: PM<sub>10</sub>  
966 concentrations, phenomenology and trends, and its relation with synoptic  
967 and mesoscale meteorology, *Atmos. Chem. Phys.*, 13, 1395–1410,  
968 doi:10.5194/acp-13-1395-2013, 2013b.
- 969 Pio, C. A., Legrand, M., Alves, C. A., Oliveira, T., Afonso, J., Caseiro, A.,  
970 Puxbaum, H., Sanchez-Ochoa, A. and Gelencsér, A.: Chemical composition  
971 of atmospheric aerosols during the 2003 summer intense forest fire period,

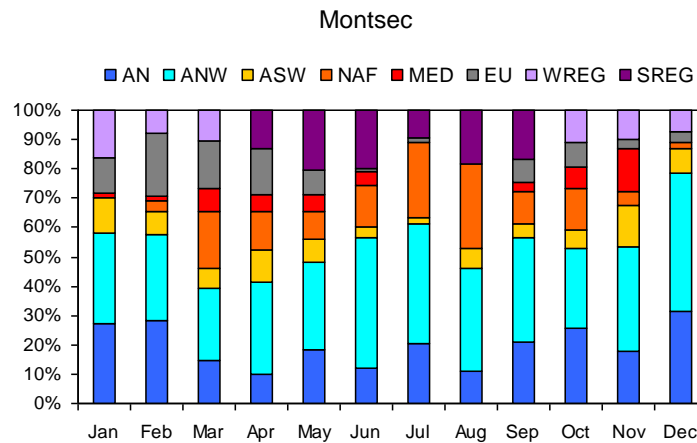
- 972 Atmos. Environ., 42, 7530–7543, doi:10.1016/j.atmosenv.2008.05.032,  
973 2008.
- 974 Pio, C., Cerqueira, M., Harrison, R. M., Nunes, T., Mirante, F., Alves, C.,  
975 Oliveira, C., Sanchez de la Campa, A., Artíñano, B. and Matos, M.: OC/EC  
976 ratio observations in Europe: Re-thinking the approach for apportionment  
977 between primary and secondary organic carbon, Atmos. Environ., 45, 6121–  
978 6132, doi:10.1016/j.atmosenv.2011.08.045, 2011.
- 979 Pöschl, U., Martin, S. T., Sinha, B., Chen, Q., Gunthe, S. S., Huffman, J. A.,  
980 Borrmann, S., Farmer, D. K., Garland, R. M., Helas, G., Jimenez, J. L., King,  
981 S. M., Manzi, A., Mikhailov, E., Pauliquevis, T., Petters, M. D., Prenni, A. J.,  
982 Roldin, P., Rose, D., Schneider, J., Su, H., Zorn, S. R., Artaxo, P. and  
983 Andreae, M. O.: Rainforest aerosols as biogenic nuclei of clouds and  
984 precipitation in the Amazon., Science, 329, 1513–6,  
985 doi:10.1126/science.1191056, 2010.
- 986 Putaud, J. P., Van Dingenen, R., Alastuey, A., Bauer, H., Birmili, W., Cyrys, J.,  
987 Flentje, H., Fuzzi, S., Gehrig, R., Hansson, H. C., Harrison, R. M.,  
988 Herrmann, H., Hitzenberger, R., Hüglin, C., Jones, A. M., Kasper-Giebl, A.,  
989 Kiss, G., Koussa, A., Kuhlbusch, T. A. J., Löschau, G., Maenhaut, W.,  
990 Molnar, A., Moreno, T., Pekkanen, J., Perrino, C., Pitz, M., Puxbaum, H.,  
991 Querol, X., Rodriguez, S., Salma, I., Schwarz, J., Smolik, J., Schneider, J.,  
992 Spindler, G., ten Brink, H., Tursic, J., Viana, M., Wiedensohler, A. and Raes,  
993 F.: A European aerosol phenomenology - 3: Physical and chemical  
994 characteristics of particulate matter from 60 rural, urban, and kerbside sites  
995 across Europe, Atmos. Environ., 44, 1308–1320,  
996 doi:10.1016/j.atmosenv.2009.12.011, 2010.
- 997 Querol, X., Alastuey, A. S., Puigercus, J. A., Mantilla, E., Miro, J. V, Lopez-  
998 soler, A., Plana, F. and Artíñano, B.: Seasonal evolution of suspended  
999 particles around a large coal-fired power station: chemical characterization,  
1000 32, 719-731, 1998.
- 1001 Querol, X., Alastuey, A., Lopez-soler, A., Plana, F. and Puigercus, J. A.: Daily  
1002 evolution of sulphate aerosols in a rural area , northeastern Spain -  
1003 elucidation of an atmospheric reservoir effect, Environ. Pollut., 105, 397–  
1004 407, doi:10.1016/S0269-7491(99)00037-8, 1999.
- 1005 Querol, X., Alastuey, A., Rodriguez, S., Plana, F., Mantilla, E. and Ruiz, C. R.:  
1006 Monitoring of PM10 and PM2.5 around primary particulate anthropogenic  
1007 emission sources, Atmos. Environ., 35, 845–858, doi:10.1016/S1352-  
1008 2310(00)00387-3, 2001.
- 1009 Querol, X., Viana, M., Alastuey, A., Amato, F., Moreno, T., Castillo, S., Pey, J.,  
1010 de la Rosa, J., Sánchez de la Campa, A., Artíñano, B., Salvador, P., García  
1011 Dos Santos, S., Fernández-Patier, R., Moreno-Grau, S., Negral, L.,  
1012 Minguillón, M. C., Monfort, E., Gil, J. I., Inza, A., Ortega, L. A., Santamaría,  
1013 J. M. and Zabalza, J.: Source origin of trace elements in PM from regional

- 1014 background, urban and industrial sites of Spain, *Atmos. Environ.*, 41, 7219–  
1015 7231, doi: 10.1016/j.atmosenv.2007.05.022, 2007.
- 1016 Querol, X., Alastuey, A., Pey, J., Cusack, M., Pérez, N., Mihalopoulos, N.,  
1017 Theodosi, C., Gerasopoulos, E., Kubilay, N. and Koçak, M.: Variability in  
1018 regional background aerosols within the Mediterranean, *Atmos. Chem.*  
1019 *Phys.*, 9, 4575–4591, doi:10.5194/acp-9-4575-2009, 2009.
- 1020 Ripoll, A., Pey, J., Minguillón, M. C., Pérez, N., Pandolfi, M., Querol, X., and  
1021 Alastuey, A.: Three years of aerosol mass, black carbon and particle number  
1022 concentrations at Montsec (southern Pyrenees, 1570 m a.s.l.), *Atmos.*  
1023 *Chem. Phys.*, 14, 4279-4295, doi:10.5194/acp-14-4279-2014, 2014.
- 1024 Rodríguez, S., Alastuey, a., Alonso-Pérez, S., Querol, X., Cuevas, E., Abreu-  
1025 Afonso, J., Viana, M., Pérez, N., Pandolfi, M. and de la Rosa, J.: Transport  
1026 of desert dust mixed with North African industrial pollutants in the subtropical  
1027 Saharan Air Layer, *Atmos. Chem. Phys.*, 11, 6663–6685, doi:10.5194/acp-  
1028 11-6663-2011, 2011.
- 1029 Rodríguez, S., Querol, X., Alastuey, A. and Mantilla, E.: Origin of high summer  
1030 PM10 and TSP concentrations at rural sites in Eastern Spain, *Atmos.*  
1031 *Environ.*, 36, 3101–3112, doi: 10.1016/S1352-2310(02)00256-X, 2002.
- 1032 Rodríguez, S., Querol, X., Alastuey, A., Viana, M.-M. and Mantilla, E.: Events  
1033 affecting levels and seasonal evolution of airborne particulate matter  
1034 concentrations in the Western Mediterranean., *Environ. Sci. Technol.*, 37,  
1035 216–222, doi:10.1021/es020106p, 2003.
- 1036 Seco, R., Peñuelas, J., Filella, I., Llusià, J., Molowny-Horas, R., Schallhart, S.,  
1037 Metzger, A., Müller, M. and Hansel, A.: Contrasting winter and summer VOC  
1038 mixing ratios at a forest site in the Western Mediterranean Basin: the effect  
1039 of local biogenic emissions, *Atmos. Chem. Phys.*, 11, 13161–13179,  
1040 doi:10.5194/acp-11-13161-2011, 2011.
- 1041 Sicard, M., Rocadenbosch, F., Reba, M. N. M., Comerón, a., Tomás, S.,  
1042 García-Vizcaino, D., Batet, O., Barrios, R., Kumar, D. and Baldasano, J. M.:  
1043 Seasonal variability of aerosol optical properties observed by means of a  
1044 Raman lidar at an EARLINET site over Northeastern Spain, *Atmos. Chem.*  
1045 *Phys.*, 11, 175–190, doi:10.5194/acp-11-175-2011, 2011.
- 1046 Takahama, S., Schwartz, R. E., Russell, L. M., Macdonald, A. M., Sharma, S.  
1047 and Leaitch, W. R.: Organic functional groups in aerosol particles from  
1048 burning and non-burning forest emissions at a high-elevation mountain site,  
1049 *Atmos. Chem. Phys.*, 11, 6367–6386, doi:10.5194/acp-11-6367-2011, 2011.
- 1050 Thurston, G. D. and Spengler, J. D.: A quantitative assessment of source  
1051 contributions to inhalable particulate matter pollution in metropolitan Boston,  
1052 *Atmos. Environ.*, 19, 9–25, 1985.

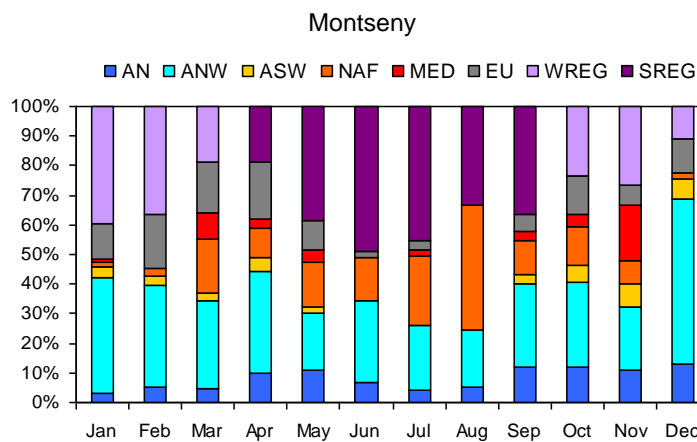
- 1053 Tositti, L., Riccio, a., Sandrini, S., Brattich, E., Baldacci, D., Parmeggiani, S.,  
1054 Cristofanelli, P. and Bonasoni, P.: Short-term climatology of PM10 at a high  
1055 altitude background station in southern Europe, *Atmos. Environ.*, 65, 142–  
1056 152, doi:10.1016/j.atmosenv.2012.10.051, 2013.
- 1057 Wall, S. M., John, W. and Ondo, J. L.: Measurement of aerosol size  
1058 distributions for nitrate and major ionic species, *Atmos. Environ.*, 22, 1649–  
1059 1656, doi:10.1016/0004-6981(88)90392-7, 1988.
- 1060 WHO, 2013. Review of evidence on health aspects of air pollution –  
1061 REVIHAAP. First Results. WHO's Regional Office for Europe,  
1062 Copenhagen, 28 pp.  
1063 [http://www.euro.who.int/\\_\\_data/assets/pdf\\_file/0020/182432/e96762-](http://www.euro.who.int/__data/assets/pdf_file/0020/182432/e96762-)  
1064 [final.pdf](http://www.euro.who.int/__data/assets/pdf_file/0020/182432/e96762-final.pdf)
- 1065 Zhuang, H., Chan, C. K., Fang, M. and Wexler, A. S.: Formation of nitrate and  
1066 non-sea-salt sulfate on coarse particles, *Atmos. Environ.*, 33, 4223–4233,  
1067 doi:10.1016/S1352-2310(99)00186-7, 1999a.
- 1068 Zhuang, H., Chan, C. K., Fang, M. and Wexler, A. S.: Size distributions of  
1069 particulate sulfate , nitrate , and ammonium at a coastal site in Hong Kong,  
1070 3, 843–853, doi: 10.1016/S1352-2310(98)00305-7, 1999b.
- 1071



1072



1073

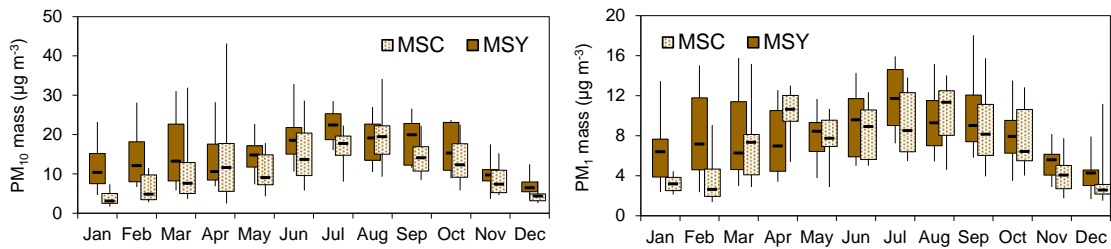


1074

1075

1076

**Fig. 1 Average frequency of air mass origin at Montsec and Montseny for the different months based on daily calculations between January 2010 and March 2013.**



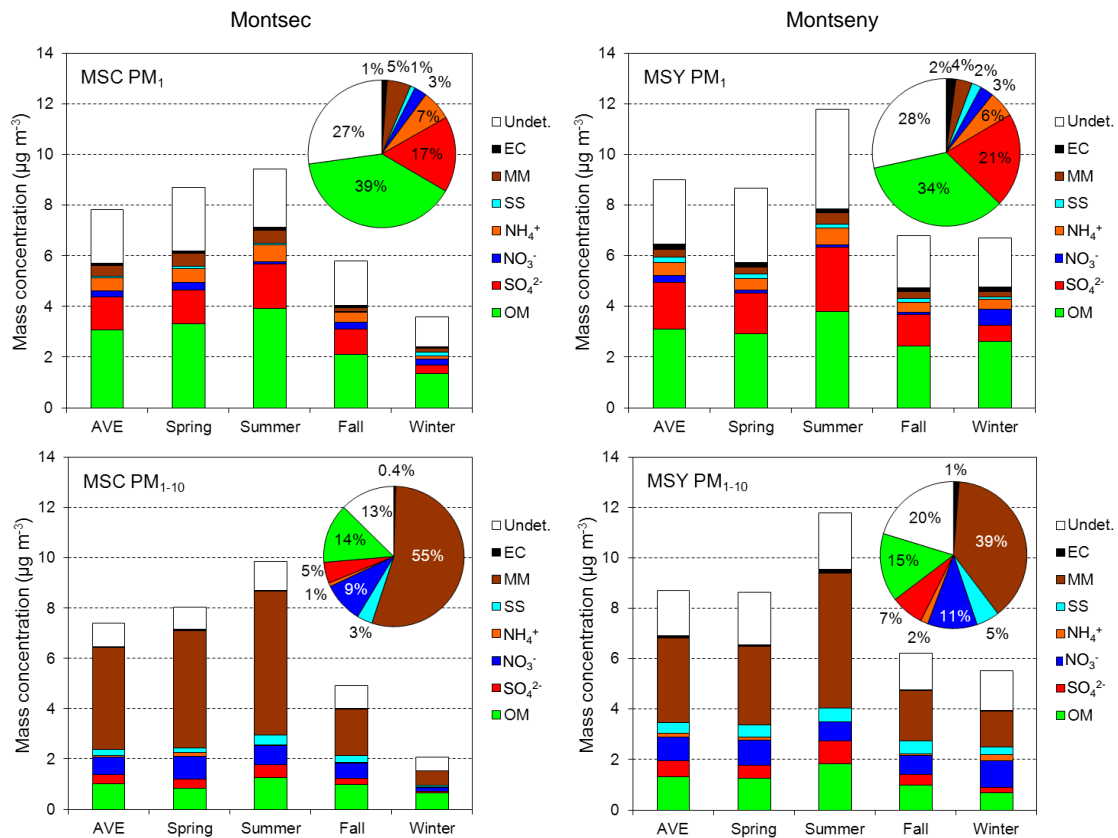
1077

1078

1079

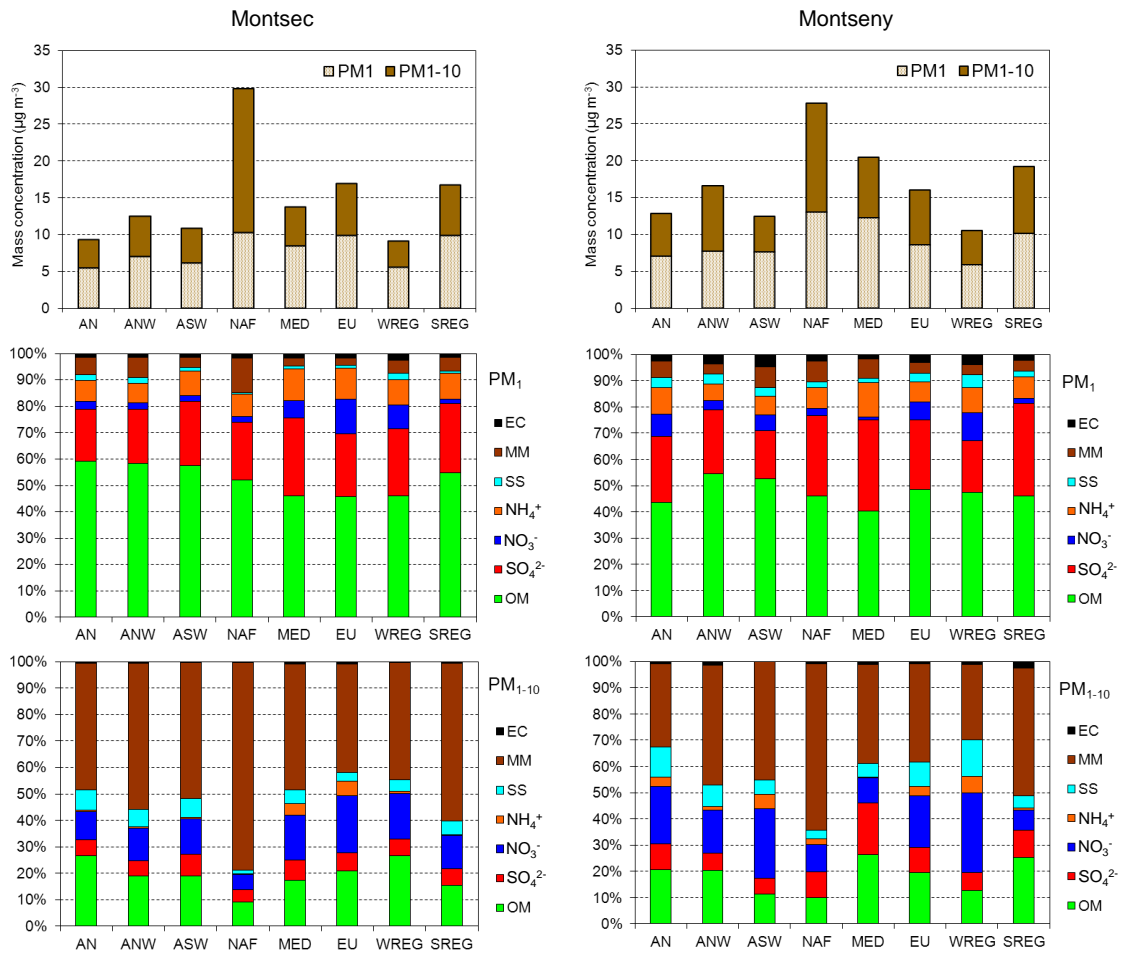
1080

**Fig. 2 Monthly median (black line within the boxes) and percentiles (5-25-75-95, boxes and whiskers) of daily PM<sub>10</sub> and PM<sub>1</sub> mass concentrations at Montsec (MSC) and Montseny (MSY) based on daily measurements between January 2010 and March 2013.**



1081  
 1082  
 1083  
 1084  
 1085  
 1086

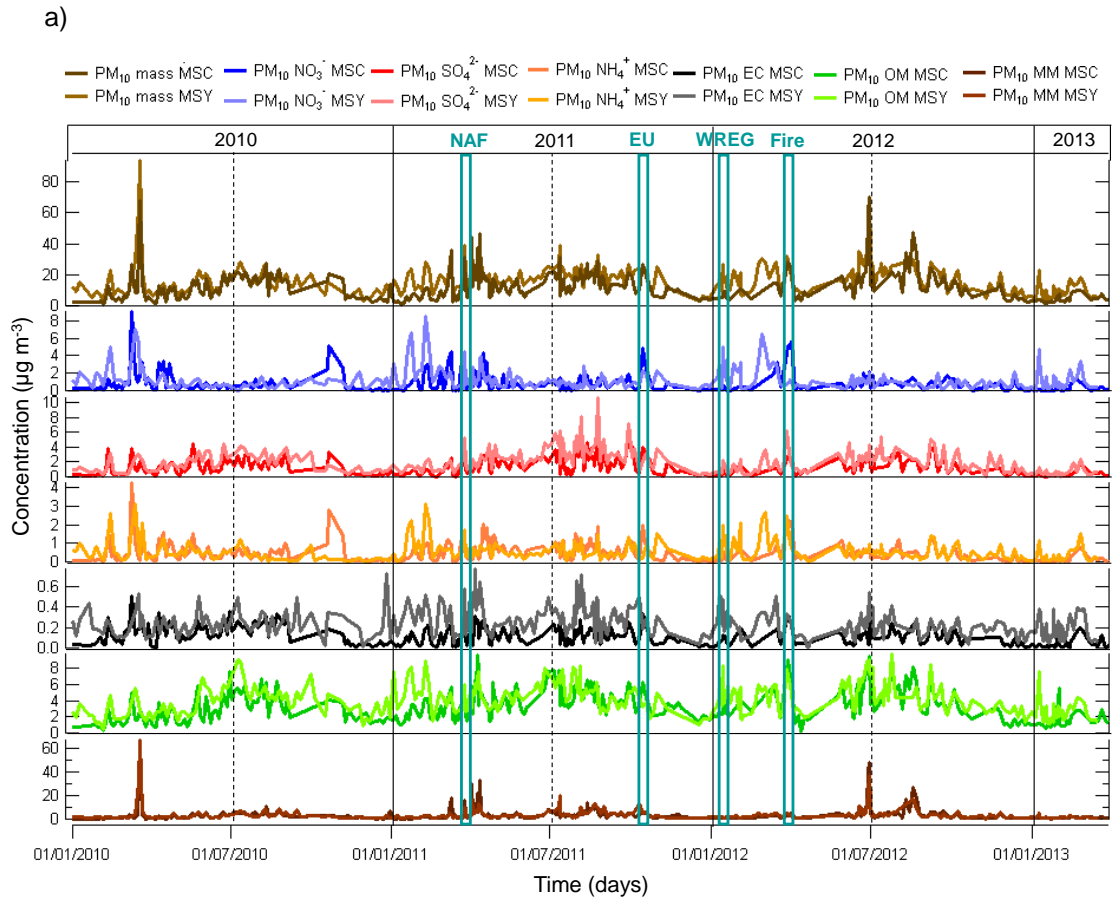
**Fig. 3** Average concentrations of aerosol major components in PM<sub>1</sub> and PM<sub>1-10</sub> fractions at Montsec and Montseny for the whole period (AVE) and for different seasons based on daily measurements between January 2010 and March 2013. Pie charts represent the average relative contribution of aerosol major components to total mass for each fraction.



1087  
 1088  
 1089  
 1090  
 1091  
 1092

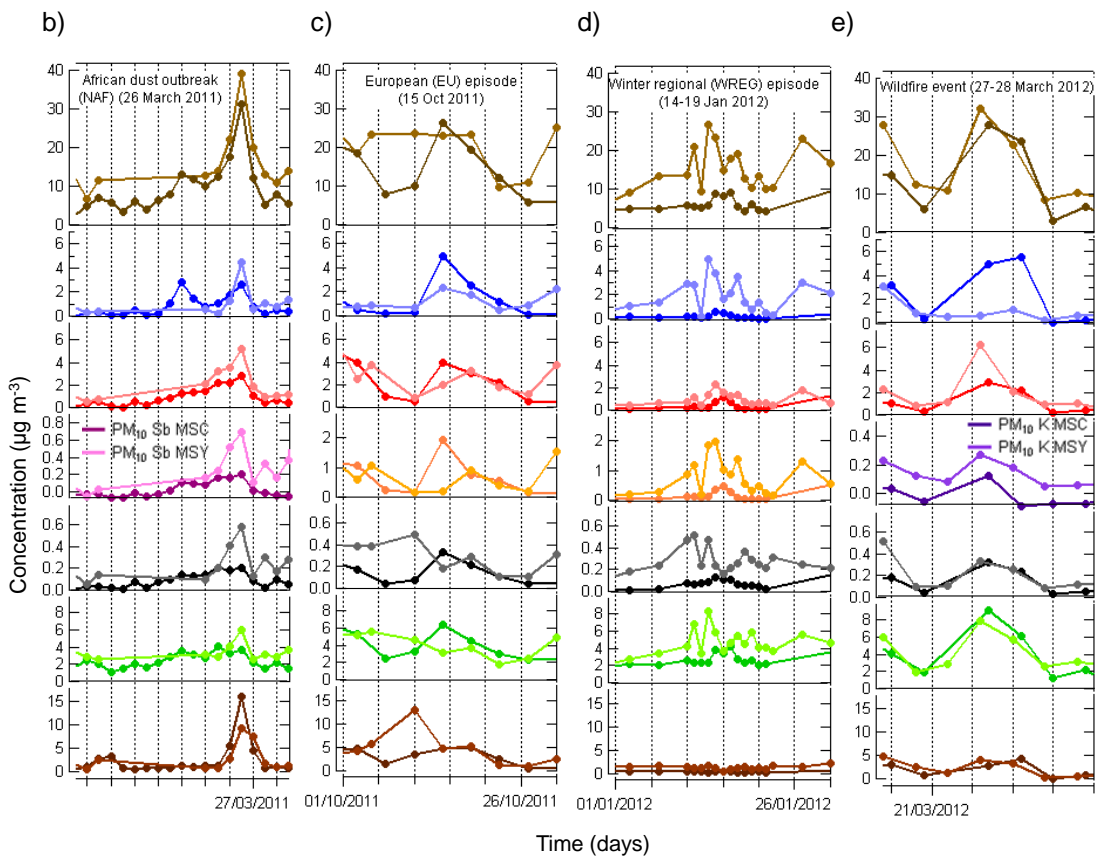
**Fig. 4 Average concentrations of PM<sub>1</sub> and PM<sub>1-10</sub> mass and relative contribution of aerosol major components in PM<sub>1</sub> and PM<sub>1-10</sub> fractions for different meteorological episodes at Montsec and Montseny based on daily measurements between January 2010 and March 2013.**

1093



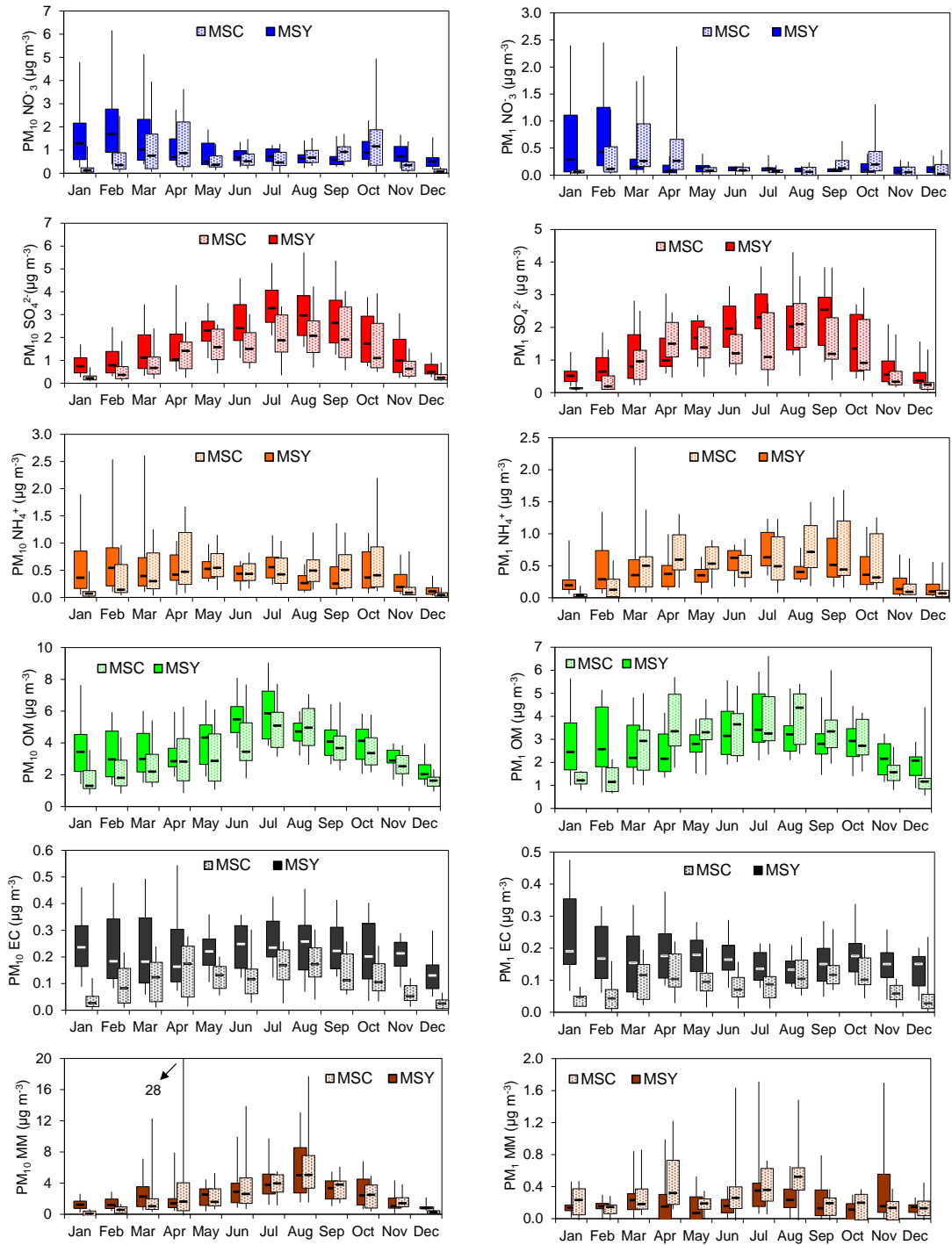
1094

1095



1096

1097            **Fig. 5 (a) Time series of daily  $PM_{10}$  mass and major  $PM_{10}$  chemical components**  
1098 **concentrations at Montsec (MSC) and Montseny (MSY) between January 2010 and March**  
1099 **2013. Green bands indicate 4 examples of different episodes affecting the study area.**  
1100 **Zoom of the 4 selected meteorological episodes: (b) African dust outbreak, (c) European**  
1101 **episode, d(d) winter regional episode, and (e) wildfire event, with daily  $PM_{10}$  mass and**  
1102  **$PM_{10}$  chemical components concentrations.**  
1103



1104  
 1105  
 1106  
 1107  
 1108

**Fig. 6** Monthly median (black line within the boxes and percentiles (5-25-75-95, boxes and whiskers) of major  $PM_{10}$  and  $PM_1$  chemical components concentrations at Montsec (MSC) and Montseny (MSY) based on daily measurements between January 2010 and March 2013.

